NTNU – Trondheim
Norwegian University of
Science and Technology

Stochastic model of mating decision control in yeast through the scaffold protein Ste5

Lisa Merete Markussen

Cell biology
Submission date: May 2013
Supervisor: Atle M. Bones, IBI
Co-supervisor: Eivind Almaas, IBT

Norwegian University of Science and Technology
Department of Biology

Stochastic model of mating decision control in yeast through the scaffold protein Ste5

Lisa Merete Markussen

Biology
Submission date: May 2013
Supervisor: Atle M. Bones, IBI
Co-supervisor: Eivind Almaas, IBT

Norwegian University of Science and Technology
Department of Biology

Acknowledgements

This work was conducted at the Department of Biology at the Norwegian University of Science and Technology (NTNU) in the period August 2011 – May 2013.
First, I would like to thank my supervisor Professor Atle M.Bones for a good collaborate and helpful comments regarding my thesis.
Following, I would like to thank my co-supervisor Professor Eivind Almaas for a very good guidance and inspiration in my master thesis. Thanks to Post. Doc. Sungmin Lee,
PhD. Marius Eidsaa , PhD. Andre Voigt, and PhD. Håvard Nedrelid for a good introduction to programming and helpful comments.
A last, I would to thank all my family and friends for believing in me and giving me moral support.

Trondheim, May, 2013

Lisa Merete Markussen

Abstract

High throughput technologies in genetics laid the foundations for systems and synthetic biology. Systems and synthetic biology became an important topic in biology research. It was used in research to investigate the behavior and relations of all elements in biological systems while it was functioning. The intracellular signal transduction pathway, where the haploid yeast *Saccharomyces cerevisiae* responds to the mating pheromone in its surroundings, is believed to be one of the best understood and studied signaling pathways in eukaryotes. In Malleshaiah *et al.* (2010) it was introduce a general model of the switch-like mating decision in the haploid yeast *S.cerevisiae*. The general model consisted of the Ptc1, Ste5, and Fus3 circuit with two-stage binding that exhibited zero-order ultrasensitivity. The model of a switch-like mating decision in the haploid yeast *S. cerevisiae* was modified in order to perform both deterministic and stochastic analysis. Deterministic analysis was conducted with mean measurements. Furthermore, stochastic simulations of the modified model were conducted. Hence, it was possible to analyze the fluctuations in the system by calculating the mean, standard deviation, coefficient of variation and fano factor. This gave an indication of the switch. It was calculated the mean values of free and bound Ste5 molecules and the amount in every single complexes. Due to an increase of the Ste5 and Fus3 molecules, the mean of free and bound Ste5 molecules were changed. By calculating the mean of bound Ste5 molecules in single complexes, the distribution of bound Ste5 molecules was about the same. The parameter values were conducted from literature, which were used in both the deterministic and stochastic simulations. The system was not affected by kinetic rate changes and thereby robust.

Sammendrag

"High throughput technologies" i genetikken la grunnlaget for system og syntetisk biologi. System og syntetisk biologi har blitt et viktig tema i biologisk forskning. Det er blitt benyttet I forskning til å undersøke oppførsel og relasjoner av alle elementer i biologiske systemer. Den intracellulære signal transduksjonsveien hvor den haploide gjærsoppen *Saccharomyces cerevisiae* responderer til formeringsferomonet i sine omgivelser, er antatt å være en av de mest studerte signalveiene i eukaryote. I Malleshaiah *et al.* (2010), ble det introdusert en generell modell av "switch-like mating decision" i den haploide soppen *S.cerevisiae*. Den generelle modellen bestod av Ptc1, Ste5 og Fus3 kretsen med to-stegs binding som viste null-ordens ultrasensitivitet. Modellen av "switch-like mating decision" i den haploide soppen *S. Cerevisiae* var modifisert for å kunne utføre både deterministisk og stokastisk analyse. Deterministisk analyse ble utført ved å måle gjennomsnittet av parameterne. Videre ble stokastisk simulering av den modifiserte modellen utført. Ved stokastisk simulering ble det mulig å analysere flukturasjoner i systemet ved å kalkulere gjennomsnitt, standardavvik, "coefficient of variation" og fano faktor. Det ble kalkulert gjennomsnittsverdier av fritt og bundet Ste5 molekyler i hvert enkelt kompleks. På grunn av økt Ste5 og Fus3 molekyler, ble gjennomsnittet av fritt og bundet Ste5 molekyler endret. Ved å kalkulerer gjennomsnittet av bundet Ste5 molekyler i enkle komplekser, var distribusjonen av bundet Ste5 molekyler den samme. Parameterverdier som er hentet fra litteraturen, ble benyttet i både deterministiske og stokastiske simuleringer. Systemet ble ikke påvirket av endrede kinetiske rater og er dermed robust.

Abbreviations

Perl script - programming language originally developed for text manipulation and now used for a wide range of tasks, e.g. network programming and system administration.

Computer terminal - an electronic or electromechanical hardware device used for entering data into, and displaying data from a computer or a computer system.

DNA - Deoxyribonucleic acid

mRNA - Messenger ribonucleic acid

iGem - International genetically engineered machine

ODE - Ordinary differential equation

GFP - Green fluorescent protein

tetR - Tetracycline repressor

IPTG - Isopropylthio-β-galactoside

GPCR - G-protein receptor activation

GEF - Guanine nucleotide exchange protein

MAPK - Mitogen-activated protein kinase

MAPKK - Mitogen-activated protein kinase kinase

MAPKKK - Mitogen-activated protein kinase kinase kinase

TrF - Transcription factor

aTc - Anhydortetracycline

ERK - Extracellular signal- regulated kinase

GDP - Guanosine diphosphate

GTP - Guanosine triphosphate

Ste5 - Pheromone-responsive MAPK scaffold protein

Fus3 - Mitogen-activated serine/threonine protein kinase

Ptc1 - Type 2C protein phosphatase

Contents

1. Introduction

1.1 Thesis objective

During the 90s, high throughput technologies in genetics laid the foundation for systems and synthetic biology. However, it was in the twentieth century systems and synthetic biology became an important topic in the biology research for investigation the behavior and relations of all elements in a particular biological system while it was functioning. In year 2000, two genetic circuits were published. One of these was the genetic toggle switch system composed of two repressors and two constitutive promoters, constructed to permit bistability an memory by Gardner *et al.* (Gardner et al., 2000). The other genetic circuit was the repressilator, a low copy number plasmid created in *Escherichia coli* (*E.coli*) coding an oscillation system by Elowitch and Leibler (Elowitz and Leibler, 2000). For biological systems, bistability can be generated by positive feedback that links output signals to their input signals. In signal transduction for the budding yeast *Saccharomyces cerevisiae* (*S.cerevisiae*), a positive feedback may create switches with an all-or-nothing decision (Huang et al., 2012, Pomerening, 2008).

In 1947, MacKay and Manney started the genetic analysis of yeast mating type with the isolation of sterile mutants that were unable to mate (Mackay and Manney, 1974a). They performed a screening among a mutagenized population of α-cells that carried a recessive drug resistance in order to find isolates that grew on selective medium containing the drug. The mutagenized population of α-cells was mixed with a large excess of a- mating cell types that carried a dominant sensitivity allele. The sterile mutant mapping of the mating type locus provided important information about its structure and function. Mackay and Manney have performed subsequent analysis to investigate the biochemical and physiological basis of the sterile phenotype of their mutants. Different methods were developed for measuring both the production of and the response to the appropriate mating pheromones (Mackay and Manney, 1974b). A-cells produce the peptide hormone a-factor, and α-cells produces the peptide hormone α-factor. As a respond to the opposite mating type pheromones, both cells undergo a morphological change, called “schmoo” formation. Schmoos have a characteristic elongated, pear-shape figure that may either grow in the direction of cells or mating pheromone of the opposite mating type. The intracellular signal transduction pathway, where the haploid yeast Saccharomyces cerevisiae (*S.cerevisiae*) respond to the mating pheromone in its

surroundings, is believed to be one of the best understood and studied signaling pathways in eukaryotes (Bardwell, 2005) (Elion, 2000).

In Malleshaiah *et al.* (2010) there was introduced a general model of the switch-like mating decision in the haploid yeast *S.cerevisiae*. The general model consisted of the Ptc1, Ste5, and Fus3 circuit with two-stage binding that exhibited zero-order ultrasensitivity (Malleshaiah et al., 2010). Assumption for the model was that only Ste5, Fus3, and Ptc1 contributed to the switch. Ste5 has four identical phosphosites that Fus3 can phosphorylate and Ptc1 can dephosphorylate. It is three types of enzyme-substrate complexes in the general model: Fus3 and Ste5 can bind to the docking motif (DM) and hence partly active, Fus3 and Ptc1 can phosphorylate/dephosphorylate the phosphosites after binding to the FM because of the two-stage binding, and Fus3 and Ptc1 can dissociate from the DM while bound to the phosphosites. Due to the zero-order ultrasensitivity, both Ste5 and Ptc1 must dissociate from DM after one phosphorylation/dephosphorylating in order to phosphorylate/dephosphorylate other phosphosites on Ste5. The nature article by Malleshaiah *et al*. (2010) is the starting point for the master thesis. The switch-like decision in the haploid yeast *S.cerevisiae* is studied and there is a focus on the stochasticity in the biological system additionally to steady-state measurement of Ste5, Fus3, and Ptc1.

The following parts will give an introduction to the fields of systems and synthetic biology, genetic circuits with a detailed description of the two genetic circuits: toggle switch and repressilator, a general modeling approaches in systems biology, differences between deterministic and stochastic systems, a description of the robustness in biological systems, and some mathematics behind the analysis.

1.2 Systems and synthetic biology

Since the ninetieth century, the process of life reached a milestone when the law of physics and chemistry explained it. The structure and physiology of living systems became a popular topic for researchers, which resulted in more detailed studies in order to reveal how the mysteries of life arises from functional and structural organization of cells and by continuous mutations and selection (Klipp et al., 2011). Engineered science started to be more important for robotically screening, quantity measuring, gene copies, enzymes in cells, and the “omics” technologies. In the twentieth century, the engineering systems became important in the biotechnology research, however biological systems were more complex and their

mechanisms were less known. Systems biology in high throughput technologies in genetics began to be well studied in the twentieth century with the attempts to investigate the behavior and relations of all the elements in a particular biological system while it was functioning. This was a new "system-oriented" biology that aims a system-level understanding of biological processes and biological networks. By this, it was possible to study the information flows of all biological levels: genomic DNA, mRNA, proteins, informational pathways, and regulatory networks. By studying system structures, system dynamics, control methods, and design methods; the study of life to help in understanding how the cellular networks work together were possible (Fu and Panke, 2009). In the recent years, a new research field called synthetic biology has emerged. Synthetic biology is not a "new" branch of science, but a new way of thinking that relies on and shares tools from the genetic engineering, bioengineering, systems biology, and many other engineering disciplines. It is the redesign of biological systems and their parts for useful and practical purposes: understanding of the life processes, generating functional modular components, and develop of novel applications and processes, respectively (Andrianantoandro et al., 2006).

1.3 Genetic circuits

As described in Sec.1.1, since the foundation of synthetic biology the study of artificial gene circuits has become more important in the recent years. Nowadays, artificial gene circuits are assumed to be the best studied system in synthetic biology (Myers, 2009). Designing artificial gene circuits are performed by inserting foreign genes into microorganism and subsequently changing their transcription and/or translation in a controlled way (Voit, 2013). A variety of artificial gene circuits approaches have been performed in the past, but one of the first working examples was the genetic toggle switch, proposed by Gardner and colleagues in 2000 (Gardner et al., 2000) to permit bistability and memory. In biological systems, bistability can be generated by positive feedback that links output signals to their input signals. In signal transduction for budding yeast, the positive feedback can create switches with an all-or-nothing decision (Huang et al., 2012, Pomerening, 2008). The genetic toggle switch system was composed of two Repressors and two constitutive Promoters. LacI Repressor was used as Repressor 2, which repressed the Promoter 2 (Ptrc-2) being inducible by isopropylthio-β-galactoside **(**IPTG) working as Inducer 2. Promoter 2 would either encode a heat inducible cI Repressor or an anhydortetracycline (aTc) inducible retR Repressor that

was able to repress Promoter 1. Given expression from Promoter 2 it will be expression of a reporter gene, in this case in the form of the *GFPmut3* gene. The schematic representation of the genetic toggle switch can be seen in figure 1a, and the vector design in figure 1b, respectively. The transcribed Repressor from the opposing promoter inhibited each Promoter. By the use of an external Inducer, the inhibition of one Repressor became possible. The system moved to a stable state; one gene was transcribed and the other was repressed. Because of the stability of the system it remained in a specific on-off state. It was not exposed to the external Inducer unless the system became forced into the second steady state by another perturbation. The bistability of the toggle switch occurred as a result of the arrangement of the repressor gene that mutually inhibited the respective Promoter. By using the construct design in *E.coli* strain JM2.300, two different stable states were possible when the Inducers were absence: one when the Promoter 1 transcribed Repressor 2, and one when Promoter 2 transcribed Repressor 1. By introducing an Inducer (chemical or physical) of the currently active Repressor, the system could reach a switch. The Inducer could permit the opposing repressor to be maximally transcribed until the originally active Promoter was stably repressed (Gardner et al., 2000, Voit, 2013).

(a) (b)

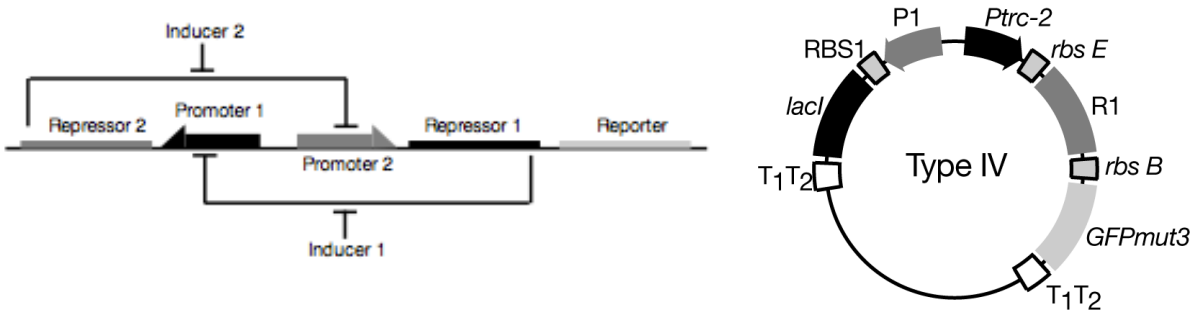

Figure 1. Toggle switch. (a) Schematic representation of a genetic toggle switch. Repressor 1 inhibits transcription from Promoter 1 and is induced by Inducer 1. Repressor 2 inhibits transcription from Promoter 2 and is induced by Inducer 2. (b) Illustration of the vector design for the toggle switch. Both figures adapted from (Gardner et al., 2000).

At the same time the genetic toggle switch was proposed by Gardner and colleagues (2000), Elowitch and Leibler created a new system called the repressilator (Elowitz and Leibler, 2000). The repressilator was a low-copy number plasmid created in *Escherichia coli* (*E.coli)* coding an oscillating system. The repressilator system was a circular negative feedback-loop

that contained a higher-copy-number reporter plasmid with a tetracycline-repressible Promoter fused to a gene coding for green fluorescent protein (GFP). Transient pulse of IPTG, an Inducer of β-galactosidace activity in bacteria, which interfered with the repression by LacI, stimulated the system. The repressilator circuit consisted of three repressor proteins (LacI-lite, tetR-lite and λcl-lite) and their corresponding Promoters ($P_L$lac01, $P_L$tet01 and λP_R). The $P_L$lac01 and $P_L$tet01 were strong repressible Promoters that contained lac- and tet operators. One of the $P_L$tet01 Promoters encodes the *λ cI-lite* gene. The λ cI-lite repressor protein can repress the Promoter λP_R that encodes the *lacI-lite* gene. The lacI-lite repressor protein can repress the Promoter $P_L$lac01 that encodes the *tetR-lite* gene. The tetR-lite repressor protein can repress both $P_L$tet01 Promoters: one encodes the *λ cI-lite* gene and the other encodes the *gfp-aav* gene, respectively. By repressing the $P_L$tet01 Promoter that encodes the *gfp-aav* gene, the expression of the reporter gene *gfp-aav* can occur. The schematic representation of the cyclical system of the repressilator can be seen in figure 2a, and an illustration of the two plasmids contained by a culture of *E.coli* strain MC 4100 to produce an oscillating behavior in figure 2b, respectively.

(a) **(b)**

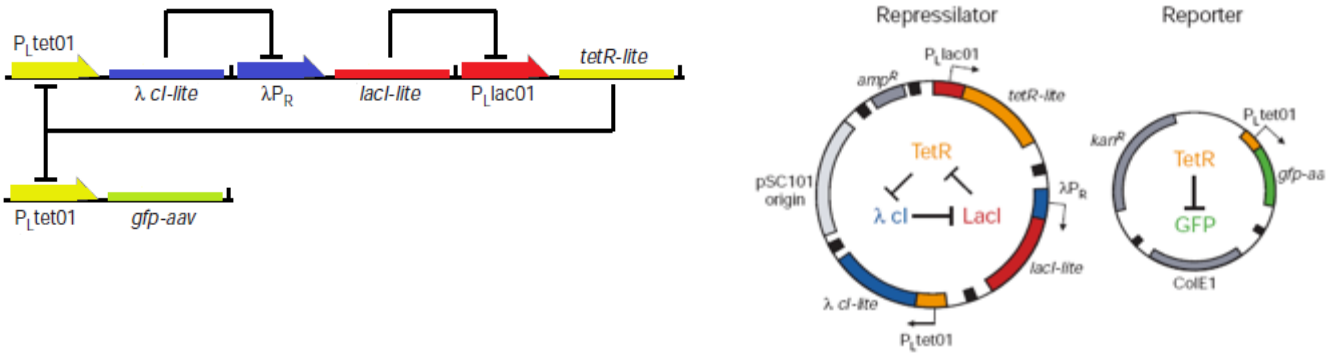

Figure 2. The repressilator. **(a)** Schematic representation of the cyclical system of the repressilator. One of the $P_L$tet01 Promoters encodes the *λ cI-lite* gene. The λ cI-lite repressor protein can repress the Promoter λP_R that encodes the *lacI-lite* gene. The lacI-lite repressor protein can repress the Promoter $P_L$lac01 that encodes the *tetR-lite* gene. The tetR-lite repressor protein can repress both $P_L$tet01 Promoters: one encodes the *λ cI-lite* gene and the other encodes the *gfp-aav* gene, and thereby the expression of the reporter *gfp-aav* gene. **(b)** Illustration of the vector design for the repressilator and the reporter. All figures adapted from (Elowitz and Leibler, 2000).

Factors like transcription rate for repressor concentration, translation rate, and the decay state of the protein and messenger RNA (mRNA) may affect the action of the network. These

parameter values can result in at least to possible outcome: the system may converge a stable steady state, or a consequently limit-cycle oscillations may occurs as a result from unstable steady state (Elowitz and Leibler, 2000, Voit, 2013).

1.4 Modeling in systems biology

Various computational methods, both for the support of network model development and for the analysis of their functionality, have shown great promising in being a research tools. Understanding the networks dynamics and predict the behavior of regulatory networks, results in less time consuming and cheaper biotechnological projects. Computational models are divided into three different classes: logical models (Boolean networks), continuous models, and stochastic models. Logical models describe the regulatory network qualitatively and thereby make it possible to understand the network functionalities under different conditions. At any point in logical models, the status of each entity in the system has a value (local state). There are two alternative levels of entity: Value one for active, or value zero for inactive. The Boolean network make is possible to study the existence of steady states or network robustness. It has already been used to study the cell-cell regulation in yeast: to analyze the relationship between the network stability, and the regulation functions in the yeast transcriptional network. Continuous models can be used when understanding and manipulation of the behaviors are depending on finer and exact molecular concentrations. The common approach for continuous modeling is by the use of ordinary differential equations (ODEs). By using real-value parameters over a continuous timescale instead of discretization that transform the numerical values into discrete ones, the data in the continuous model are more accurate than in the logical model. Stochastic models are also called single-molecule level models because the network is an interaction between individual molecules, which gives an explanation of the relationship between stochasticity and gene regulation. Due to stochastic components in biological networks, every network will have different behavior even though the initial conditions are the same. A stochastic simulator like Cain (Mauch, 2011), can simulate a model by using algorithms made for the stochastic simulation of coupled chemical reactions, like the Gillespie Direct (Gillespie, 1976) or the Gibson-Bruck algorithms (Gibson and Bruck, 2000). Additionally, regulatory networks are often affected by “noise”. With a large amount of molecules for each species, little or no concentration changes can be observed. Significant stochastic effects can be seen when there is a small amount of molecules. (Karlebach and Shamir, 2008).

1.5 Deterministic and stochastic behavior of chemical systems

Two different mathematically formalisms can describe the time behavior of a homogenous chemical system: deterministic and stochastic. The deterministic approach regards the time of evolution as a continuous and predictable process with no involved randomness in the future states of the system. Time of evolution is governed by a set of coupled ODEs (Gillespie, 1977). In deterministic simulations, rate equations are often used in chemical reactions to link the reactions rates with pressure or concentrations of the reactants or parameters. In stochastic simulations, the rate equations are not taken into account for describing the mRNA and protein abundance. Hence, the deterministic approach is not able to capture the potentially significant effects of factors that can cause the stochasticity in gene expression (Kærn et al., 2005). Stochasticity is a non-deterministic approach because the next state is not determined by the previous state due to fluctuations in mRNA/protein numbers, internal noise, and external noise. The stochasticity approach regards the time evolution as a random-walk process governed by single differential equations (Gillespie, 1977). Stochastic simulations consider a clearly random formation and decay of multicomponent complexes of single molecules. It is possibility to predict the pattern of for example the signal protein production that can determine switching delays (McAdams and Arkin, 1997).

By calculating the mean and standard deviation of a system in its steady state, quantification of the level of noise in a variable is possible. There are different methods to measure stochasticity, but two widely used methods are the coefficient of variation (CoV) and the fano factor (F) (Zulliger and Aitken, 1970). CoV and fano factor are measurements of the magnitude fluctuations in a system. CoV is an attractive statistic tool because it can permit the comparison of variants free from scale effects; i.e., it is dimensionless (Brown, 1998) It measures the relations between the standard deviation and mean. Fano factor measures the relation between the CoV multiplied with the standard deviation (Zulliger and Aitken, 1970). The equation of the coefficient of variation and fano factor yields

$$\mathrm{CoV} = \sigma / \bar{x} \tag{1}$$

$$\mathrm{F} = \sigma^2 / \bar{x} \tag{2}$$

where σ is the standard deviation and $\bar{x}$ is the mean (Brown, 1998) (Zulliger and Aitken, 1970). In order to model the effect of the stochasticity in biological systems, stochastic

models have been developed, described in Sec. 1.4., and there have been developed software to simulate such models, described in Sec. 2.1.

1.6 Robustness in biological systems

Hiroaki Kitano defines robustness as "a property that allows a system to maintain its functions against internal and external perturbations" (Kitano, 2004). Robustness is an essential feature of biological systems due to the robust variety of levels from genetic switches to physiological reactions (Kitano, 2002a). To attain an in-depth biological and system-level understanding, it is important to understand the principles and mechanisms that underlie the biological robustness. The observable phenomena that characterize the robust systems are adaption, parameter insensitivity, and graceful degradation. Adaption indicates the ability to cope with environmental changes, and parameter insensitivity indicates the insensitivity for a system to specific kinetic parameters. At last graceful degradation, which reflects how the slow degradation of a system functions after it has been damaged, rather than catastrophic failure.

Robustness is attained in engineering systems by using a system control, redundancy, structural stability, and modularity. Approaches used in engineering systems can be found in biological systems as well. Both negative and positive feedback constitutes the system control to obtain a robust dynamic response. The dynamic response is observed in several dynamic networks: the cell cycle, the circadian clock, and chemotaxis. Bacterial chemotaxis is a well-studied example of robust adaption that uses negative feedback in order to attain chemotaxis as a response to stimuli. Robustness is achieved by positive feedback, which amplifies the stimuli in order to distinguish the activation level of the downstream pathway from a non-stimulated state. Signal transduction is an example where positive feedback is used to achieve a switch-like behavior of the system due to stimuli amplification. Stimulations initiate a new state of the system, which is more robust against noise and fluctuations (Kitano, 2004). Redundancy is where similar or identical components with equal functions are introduced for backup due to component fail. Structural stability is where the intrinsic mechanisms are built to promote stability, and decoupling separates the variations in the low-level from the high-level functions. Hsp90 (heat shock protein 90) is a chaperone protein, which fixes mis-folded proteins and decouples genetic variations by environmental stresses, thus provides a genetic buffer against mutations. Using a genetic buffer, decoupling of a genotype from a phenotype

is possible; additionally to provide the robustness to cope with the mutations while a degree of the genetic diversity is maintained. Modularity is an effective mechanism to avoid or minimize failure in systems that contain local perturbations and damages, hence prevent system-catastrophes. By designing and studying biological systems, these properties will be able to explain the robustness of the system (Kitano, 2002b, Kitano, 2004).

1.7 Mathematical approaches

The mathematical approach explained by Steve H. Strogatz in "Nonlinear Dynamics and Chaos" (2001) (Strogatz, 2001) is the basis for the mathematical theory.

1.7.1 Differential equations

Strogatz says "differential equations describe the evolution of systems in continuous time" (Strogatz, 2001). Differential equations are mathematical equations of an unknown function of one or several variables. The variables relates to the function itself or its derivate of different order. The main distinction of differential equations (DEs) is between ordinary- and partial equations. Ordinary differential equations (ODEs) are differential equations where the unknown function (dependent variables) involves only one independent variable, and partial equations (PDEs) involves several independent variables. Differential equations are divided into an nth-order system. The classification depend on the order of the highest derivate of the independent variable. First order DEs can be written in the form

$$\frac{dy}{dx} = F(x,y) \qquad (3)$$

where F(x,y) is a given expression that involves the independent variable x and the dependent variable y. Second order DEs is an equation that involves the second derivate. Second order DEs can be written in the form

$$x_1 = ax_1 + bx_2$$
$$x_2 = cx_1 + dx_2 \qquad (4)$$

where a, b, c, and d are parameters. Ordinary and partial DEs are further divided into linear and non-linear equations. Linear equations are linear in the unknown function and in its

derivate, opposite of non-linear equations. Linear DEs can be divided into homogenous and heterogeneous subclasses. Homogenous linear DEs do not contain differential denomination for both coefficients of the differential dx and dy, opposite of heterogeneous DEs. (Strogatz, 2001).

1.7.2 Steady-state kinetics

If steady state exists, the right hand side of the ODE is set to be equal to zero. The steady state represents the equilibrium solution where the time derivative is zero. In biological terms, steady states solutions represent the system behavior after time has elapsed and initial fluctuations have died out. Hence, the rates of production of x are balanced by the rates of destruction of x in the biological circuit. Fix points in the steady state represents the equilibrium solutions. The equilibrium is stable if small disturbances are reduced and damp out in time, thus gives stable fix points. Unstable equilibrium occurs when the disturbances grows with time, thus gives unstable fix points (Strogatz, 2001). Illustration of steady state is shown in figure 3.

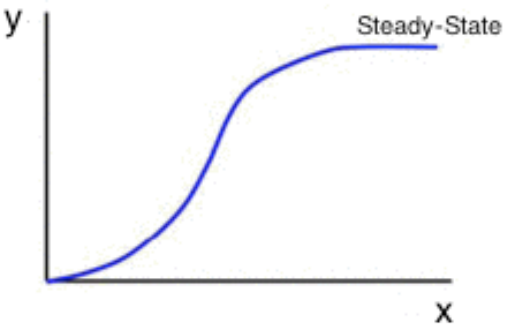

Figure 3. **Steady state kinetics**. Steady state occurs when the fix points have accomplished the equilibrium solutions. From (Strogatz, 2001).

1.7.3 Linearity in two-dimensional systems

The definition of a two-dimensional linear system, mentioned in Sec. 1.7.1, is stated as

$$\dot{x}_1 = ax_1 + bx_2$$
$$\dot{x}_2 = cx_1 + dx_2 \qquad (5)$$

where the dot notation represent the d/dt. By using boldface to denote vectors, the system can be written in the matrix form as

$$\dot{x} = Ax \tag{6}$$

where

$$A = \begin{pmatrix} a & b \\ c & d \end{pmatrix} \quad \text{and} \quad x = \begin{pmatrix} x_1 \\ x_2 \end{pmatrix} \tag{7}$$

the solution of a two-dimensional linear system can be illustrated as trajectories in a phase plane by making a phase portrait. In the phase portrait, the trajectories have a direction according to their relation to the fix point, x*. Fix points control the phase portrait and the fix points, x*, for a system are a value of x that satisfy the Ax = 0, which means that both time derivatives are zero. In a linear system, the point x*= 0 will always be a fix point. The fix points can have different behaviors as; nodes, spirals, centers, non-isolated fix points, star nodes, degenerate nodes, and saddle points. Further, their stability can either be stable or unstable, except saddle points that can only be unstable. To classify the fix points for a two-dimensional system linear system, $\dot{x} = Ax$, trace (τ) and the determinant (Δ) must be calculated for the matrix A. Trace and the determinant can be found by

$$\tau = a + d \tag{8}$$

$$\Delta = ad - bc \tag{9}$$

and using figure 4, fix points in a phase plane can be classified. From these calculations and predictions it is possible to create a phase portrait of the system. After the fix points are classified, it is possible to calculate the eigenvector of A with the corresponding eigenvalue in order to classify all the possible phase portraits that can occur in the system. Methods for calculating the eigenvector and eigenvalue can be found in the literature, like “Nonlinear Dynamics and Chaos” by Steven H. Strogatz (2001) (Strogatz, 2001).

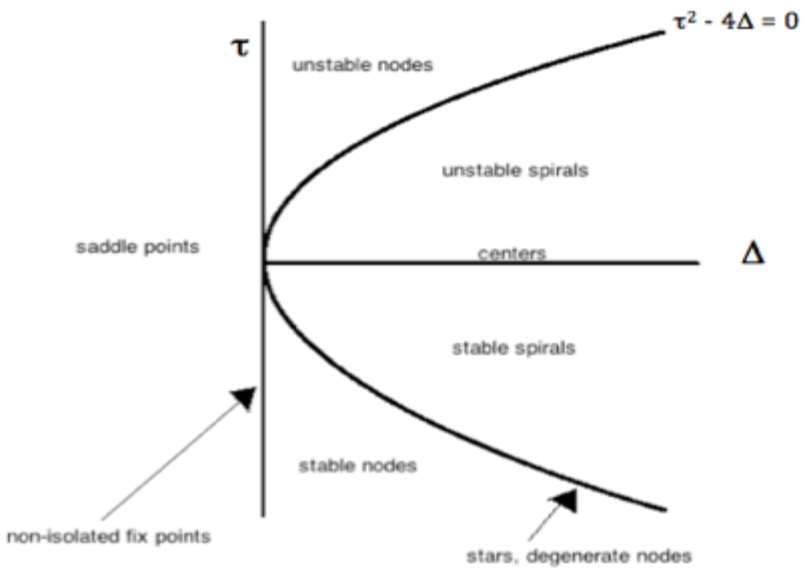

Figure 4. Classification of the fix points from the trace (τ) and the determinant (Δ) values. The figure illustrates the major types of fix points and their stability on a single diagram. The vertical axes are the trace (τ) and the horizontal axes are the determinant (Δ). Saddle points, nodes, and spirals occur in the large open regions of the (τ,Δ) plane. Centers occur along the horizontal axes (the determinant) and non-isolated fix points occur along the vertical axes (the trace). Stars, and degenerate nodes occur along the curve in the (τ,Δ) plane. The curve is $\tau^2 - 4\Delta = 0$. Spirals satisfy $\tau^2 - 4\Delta < 0$, nodes satisfy $\tau^2 - 4\Delta > 0$ and parabola satisfy $\tau^2 - 4\Delta = 0$. The parabola includes star nodes and degenerate nodes. From (Strogatz, 2001).

1.7.4 Non-linearity in two-dimensional systems

Non-linear systems can be written as a vector field on the phase plane as

$$\dot{x}_1 = f_1(x_1, x_2)$$
$$\dot{x}_2 = f_2(x_1, x_2) \qquad (13)$$

where f_1 and f_2 are the given functions. The general form can be further written as

$$\dot{x} = f(x) \qquad (14)$$

where $\dot{x}$ indicate $\dot{x}_1$ and $\dot{x}_2$, and f(x) indicates $f_1(x)$ and $f_2(x)$. A point in the phase plane is symbolized as x, and x is represented as the velocity vector at that point. The system described in Eq. (13) can be linearized to

$$\begin{pmatrix}\dot{u}\\ \dot{v}\end{pmatrix} = \begin{pmatrix}\frac{\partial f}{\partial x} & \frac{\partial f}{\partial y}\\ \frac{\partial g}{\partial x} & \frac{\partial g}{\partial y}\end{pmatrix}\begin{pmatrix}u\\ v\end{pmatrix} \quad (15)$$

where

$$A = \begin{pmatrix}\frac{\partial f}{\partial x} & \frac{\partial f}{\partial y}\\ \frac{\partial g}{\partial x} & \frac{\partial g}{\partial y}\end{pmatrix}(x^*,y^*) \quad (16)$$

A is the Jacobian matrix. The Jacobian matrix can be used to classify fixed points for the system, same methods as described for fixed points classification for linear systems in Sec. 1.7.3. The classification of fixed point in figure 4 for linear systems is described as non-isolated fixed points, star nodes, centers, star nodes and degenerate nodes are borderline cases. For non-linear systems, fixed points based solely on the Jacobian are not necessarily correct. Methods for the correct characterization of borderline cases for non-linear systems can be found in the literature "Nonlinear Dynamics and Chaos" by Steven H.Strogatz (Strogatz, 2001).

1.7.5 Bifurcations

By altering parameters in DEs, fix point can be created, destroyed, or their stability can be changed. Such qualitative changes are called bifurcations, leading to different fix point behavior. Bifurcation points are where the changes of the parameter values occur and it can be in both system, ODEs and PDEs. The bifurcation diagram displays the qualitative information about the equilibrium in a system as the parameter changes. Each parameter change in the equation produces one phase line diagram. Two-dimensional stack of the phase line is the bifurcation diagram. The stable solutions are drawn with a solid line and the unstable solutions with a dotted line, respectively. An example of a bifurcation in a scientifically way is weight placed on top of a beam. If a small weight is place on top of the beam, the beam will manage to support the load and stand vertically. When the load is too heavy it will not manage the vertical position, and the beam will buckle. Bifurcations in first-order system are divided into several mechanisms. There are different bifurcation mechanisms like saddle-

node, transcritical, and pitchfork. The mechanism, which will be further described, is saddle-node bifurcation (Strogatz, 2001).

1.7.6 Saddle-node bifurcation

Saddle-node bifurcation is the basic mechanism of creating and destroying fix points. Two fix points will move towards each other, collide, and destroy each other, due to varied parameters. The following first order DE

$$\dot{x} = \mathrm{r} + x^2 \qquad (17)$$

is an example of a saddle-node bifurcation. The parameter (r) can be negative, zero or positive. Negative parameter ($r < 0$) gives two fix points, one stable and one unstable. The two fix points will move toward each other when the parameter approach zero. If the parameter is equal zero ($r = 0$), the fix points will collide causing a half stable fix point. Positive parameter ($r > 0$) leads to none fix points due to the parameter has vanished, and they do not cross the x-axes (Strogatz, 2001). Graphs with negative, zero, and positive parameters are illustrated in figure 5, respectively.

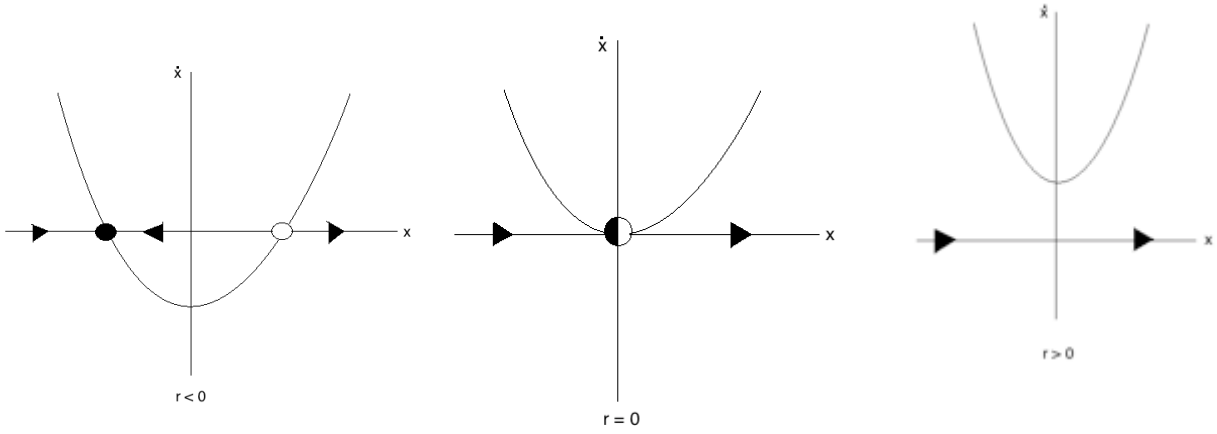

Figure 5. Saddle-node bifurcation. Illustrated graphs with negative, zero, and positive parameters. The black arrows on the x-axes indicate the direction of the flow. The dots on the x-axes indicate the stability of the fix points; black dots are stable, dots with black and white color are half-stable, and non-colored dots are unstable. The negative parameter gives two fix points, one stable and one unstable. The parameter equal zero gives one half stable fix point because the fix points have collide. The positive parameter gives no fix points since the parameter does not cross the x-axes. From (Strogatz, 2001).

As mentioned, a bifurcation diagram displays the qualitative information about the equilibrium in a system as the parameter changes. The bifurcation diagram for the saddle-node bifurcation with stable and unstable fix points can be seen in figure 6.

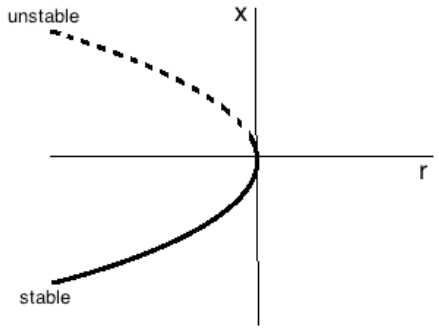

Figure 6. Saddle-node bifurcation diagram. The solid line indicates the stable fix points and the broken line indicate the unstable fix points. From (Strogatz, 2001).

1.8.1 Saccharomyces Cerevisiae

For commercial use, the yeast S.*cerevisiae* is known as the brewer´s or bakers yeast, and as budding yeast for its mode of cell division. Yeast have two different mating types, a (genotype MATa) and α (genotype MATα) (Bardwell, 2005). The two haploid cells, MATa and MATα, secrete the mating factor a- and α-factor pheromone, respectively. The pheromone binds to a specific cell-surface receptor that belongs to a G-protein-coupled receptor superfamily. The a-factor pheromone binds to the Ste3 receptor and the α-factor pheromone binds to the Ste2 receptor. By binding to its specific receptor embedded in the plasma membrane on an a- or a α- cell, the receptor undergoes a conformational change. Receptor binding enables activation of the heterotrimeric GTP-binding protein (G-protein). After G-protein binding, an activation of a MAPK signaling protein network occurs (Malleshaiah et al., 2010). Activated Fus3 can either activate Ste12, resulting in an activation of pheromone response genes, or activate Far 1, resulting in a cell cycle arrest (Montelone, 2002). Binding of a α-factor to a Ste2 receptor result to a polarized recipient cell that undergoes a morphological change, which gives a “shmoo” shape. Under normal circumstances the “shmoo” tip is directed towards an amorous α-cell located nearby, but in the presence of an α-factor gradient, the a-cell “shmoo tip” is directed to the highest concentration of the signal molecule (Alberts, 2008). Shmooing is a switch-like response that

occurs when two cells of opposite mating type become close enough, and when the pheromone concentration reaches a threshold (Malleshaiah et al., 2010). Model of the signaling transduction pathway for response to pheromone in *S.cerevisiae* can be seen in figure 13.

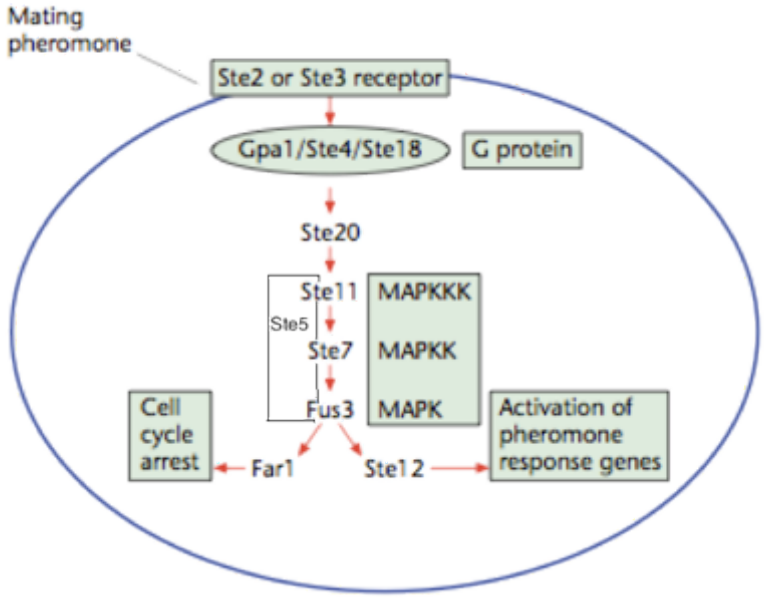

Figure 13. Signal transduction pathway in *S.cerevisiae*. The mating pheromone can either be an a- or a α-factor which binds to their specific cell-surface receptor Ste2 or Ste3. The receptor activates the heterotrimeric GTP-binding protein (G-protein), which activates several signal proteins and the mitogen-activated protein kinase (MAPK). Activated Fus3 can either activate Ste12, resulting in an activation of pheromone response genes or activate Far 1, resulting in a cell cycle arrest. From (Montelone, 2002).

1.8.2 G-protein receptor activation and signal complexes

Activation of the specific G-protein coupled receptor (GPCR) is initiated by a pheromone. α-factor pheromone binds to a specific G-protein receptor, called Ste2, on an a –cell. G-protein coupled receptors (GPCRs) are the largest family of cell-surface receptors that mediates response to signals from other cells. It is composed of three protein subunits: α-, β- and γ. In an unstimulated state where the mating factors are not bound to the receptor, the α subunit is bound to a guanosine diphosphate (GDP) and thus inactive. Binding of a pheromone factor to its specific GPCR activates the G-protein and it acts like a guanine nucleotide exchange factor (GEF). It induces the α-subunit to release its bound guanosine diphosphate (GDP) and binds guanosine triphosphate (GTP) instead. This conformational change in the G-protein contributes

to the activation of the G-protein. When the G protein is activated, the α-subunit became loosely bound to the β- and γ complex (Alberts, 2008). The membrane-bound β- and γ complex then transmit the signal by binding to three different effectors: a Ste5/Ste11 complex; Ste20 protein kinase, and a Far1/Cdc 24 complex. By binding the β- and γ complex to the different effectors, Ste20 and Ste11 became closer to each other and thereby transmit the signal further downstream (Kofahl and Klipp, 2004). The Ste20 protein kinase is the first β- and γ complex effectors and is attached to the β- and γ complex by a short motif in the C-terminal of Ste20. Binding of Ste20-Cdc42 is necessary to localize the Ste20 at the membrane. Ste5 is a protein that has no catalytic activity, but serves as a scaffold protein. It binds the intracellular signaling proteins: β-complexes; Ste11; Ste7, and Fus3, into a signaling complex. The third effector is the Far1/Cdc24 complex. A domain in the N-terminal of Far1 binds to the β- and γ complex while a domain in the C-terminal of Far1 binds to Cdc24, thereby acting as an adaptor for Cdc42 activation. Cdc24 acts like a GEF for Cdc42. Far1 helps to bring Cdc24GEF to the plasma membrane (PM) where the substrate of Cdc24, called Cdc42, is hanging. The Cdc24 acts on Cdc42 to promote an exchange of GDP to GTP. The GTP-bound Cdc42 is then able to bind several effectors involved in the cell polarity regulation and Ste20 protein kinase. The binding of β- and γ complex to Cdc24 and Cdc42 is responsible for the bud formation when the yeast cells forms a “shmoo tip” (Bardwell, 2005).

1.8.3 MAPK-cascade and scaffold protein Ste5

The Ste5 function as a scaffold protein, and it is dependent of a MAPK cascade to pursue the pheromone signal further downstream. MAPK cascades are found in all eucaryotes and they contribute to the regulation of different responses. The MAPK cascade consists of a set of three protein kinases, starting from the bottom and working upwards. In the MAPK cascade, there is a MAPK activity that phosphorylates and activates the protein kinases (Bardwell, 2005). The mitogen-activated protein kinase kinase kinase (MAPKKK) is STE11, the mitogen-activated protein kinase kinase (MAPKK) is Ste7, and Fus3 is a MAPK. Ste11 is phosphorylated and activated by Ste20, which activates the MAPK kinase function. Activated Ste11 phosphorylates and activates Ste7, and activated Ste7 phosphorylates Fus3 (Kofahl and Klipp, 2004).

1.8.4 Active Fus3 and Ptc1

Phosphorylated Fus3 is not fully active and is unable to detach from the scaffold protein Ste5. To be fully activated and released from Ste5, all four phosphosites at the scaffold protein Ste5 needs to be dephosphorylated by a serine/threonine phosphatase, Ptc1. Ptc1 has a α-factor dependent activity that is essential for "shmooing". Increasing the α-factor induces more Ptc1 to Ste5, phosphorylation of Ste5 and consequent dissociation of the Fus3-Ste5 complex, resulting in more "shmooing". Deletion of Ptc1 prevents "shmooing" and reduces activation of Fus3, while overexpression of Ptc1 enhances both. Phosphorylated Fus3 binds to Ste5 by a two-stage binding action. Fus3 must first bind to its docking motif on Ste5 before it has the ability to bind and phosphorylate phosphosites on Ste5. Same as Fus3, Ptc1 binds to Ste5 by a two-stage binding action. Ptc1 must first bind to its docking docking motif on Ste5 before it can dephosphorylate the phosphosites on Ste5. Two-stage binding on Ste5 causes a competition between Fus3 and Ptc1. An illustration of the two-stage binding of Fus3 and Ptc1 on Ste5 is illustrated in figure 14.

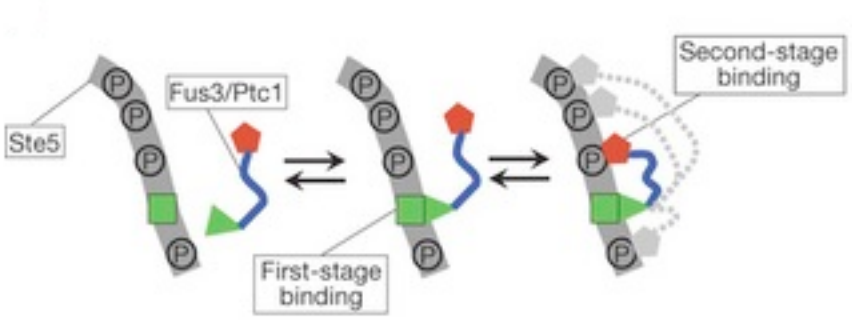

Figure 14. Two-stage binding. Fus3 and Ptc1 must first bind to separate docking motifs on Ste5 (first-stage binding) before they can phosphorylate/dephosphorylate the phosphosites on Ste5 (second-stage binding). From (Malleshaiah et al., 2010).

Dephosphorylation of the four phosphosites by Ptc1 is necessary to disrupt the Fus3-Ste5 complex to achieve a full activation of Fus3. Activated Fus3 can either activate Ste12, resulting in an activation of pheromone response genes or activate Far 1, resulting in a cell cycle arrest. When the pheromone concentration reaches a threshold, a small increase of Ptc1 causes a large increase in unphosphorylated Ste5. Fus3 is saturated, but Ptc1 is working near its maximum rate, thereby Fus3 is unable to compete with Ptc1. This results in a sharp, ultrasensitive drop in the level of Ste5 phosphorylation and Fus3 undergoes a switch-like dissociation. The sharpness of the switch is robust to changes in the Ptc1 concentration for

both the fraction of cells that “shmoo” and the binding of Fus3 to Ste5. The number of active phosphosites on Ste5 controls the sharpness of the Fus3-Ste5 interaction and the “shmoo” response. The switch indicates a reduction of the Fus3 affinity to Ste5 before the Fus3-Ste5 complex reaches the steady state (Malleshaiah et al., 2010).

2. Material and methods

2.1 Cain – Genetic circular analysis

Cain is a simulator that can be used to perform stochastic and deterministic simulations of different chemical reactions, described in Sec 1.4. Both deterministic and stochastic simulations methods of the genetic circular model were made in Cain and further exported to Matlab. For the deterministic simulation method, it was performed by numerically integrating ODEs by the Cash-Karp variant of the Runge-Kutta method. For the stochastic method, it was performed by the Gillespie method. By using a Perl Script (programming language), the exported model was modified (Mauch, 2011).

2.2 Matlab – Language of technical computering

Matlab is a high-level language and interactive environment for several tasks: numerical computation, visualization, and programming, respectively (Attaway, 2011). The simulation results of the modified model were exported into Matlab. The results were plotted in diagrams and the mean was observed for both deterministic and stochastic analysis. Additionally, for stochastic measurements, the standard deviation, coefficient of variation (CoV) and the fano factor (F) were calculated, described in Sec 1.5.

3. Result

3.1 General model description

From the signaling mating system in S.cerevisiae, a modified model of the interaction between Ptc1 and Fus3 at the scaffold protein Ste5 has been made. The analyzed system is the switch-like decision in the scaffold protein Ste5, from Malleshaiah et al. (Malleshaiah et al., 2010). The modified model consists of a Ste5, Fus3, and Ptc1 circuit with two-stage binding that exhibits zero-order ultrasensitivity. The scaffold protein Ste5 has four identical phoshosites. It is specified four different forms of the scaffold protein Ste5, denoted S0, S1, S2, S3, and S4. The unbound form S0 has no phosphorylated phosphosites. The remaining bound forms have one, two, three, or four phosphorylated phosphosites. Fus3 and Ptc1 compete in phosphorylation and dephosphorylation of the four phosphosites at the scaffold protein Ste5, leading to the switch. It is specified three different forms of Ste5-Fus3 complexes and Ste5-Ptc1 complexes, respectively. Fus3_Ste5n_0 denotes a complex where Fus3 is only bound to the DM, Fus3_Ste5n_1 denotes a complex where Fus3 is bound to the DM and a phosphosite, and Fus3_Ste5n_2 denotes a complex where Fus3 is only bound to a phosphosite. Ste5-Ptc1 complexes have the same forms denoted by Ptc1_Ste5n_0, Ptc1_Ste5n_1, and Ptc1_Ste5n_2. Green arrows indicates that both Fus3 and Ptc1 must bind to the DM on Ste5 and the blue and red arrows indicates that Fus3 or Ptc1 are bound to Ste5 DM and are engaged in enzymatic reactions with the phosphosites. Additionally, enzymes that are interacting with the phosphosites are highlighted in orange. The modified model is illustrated in figure 15.

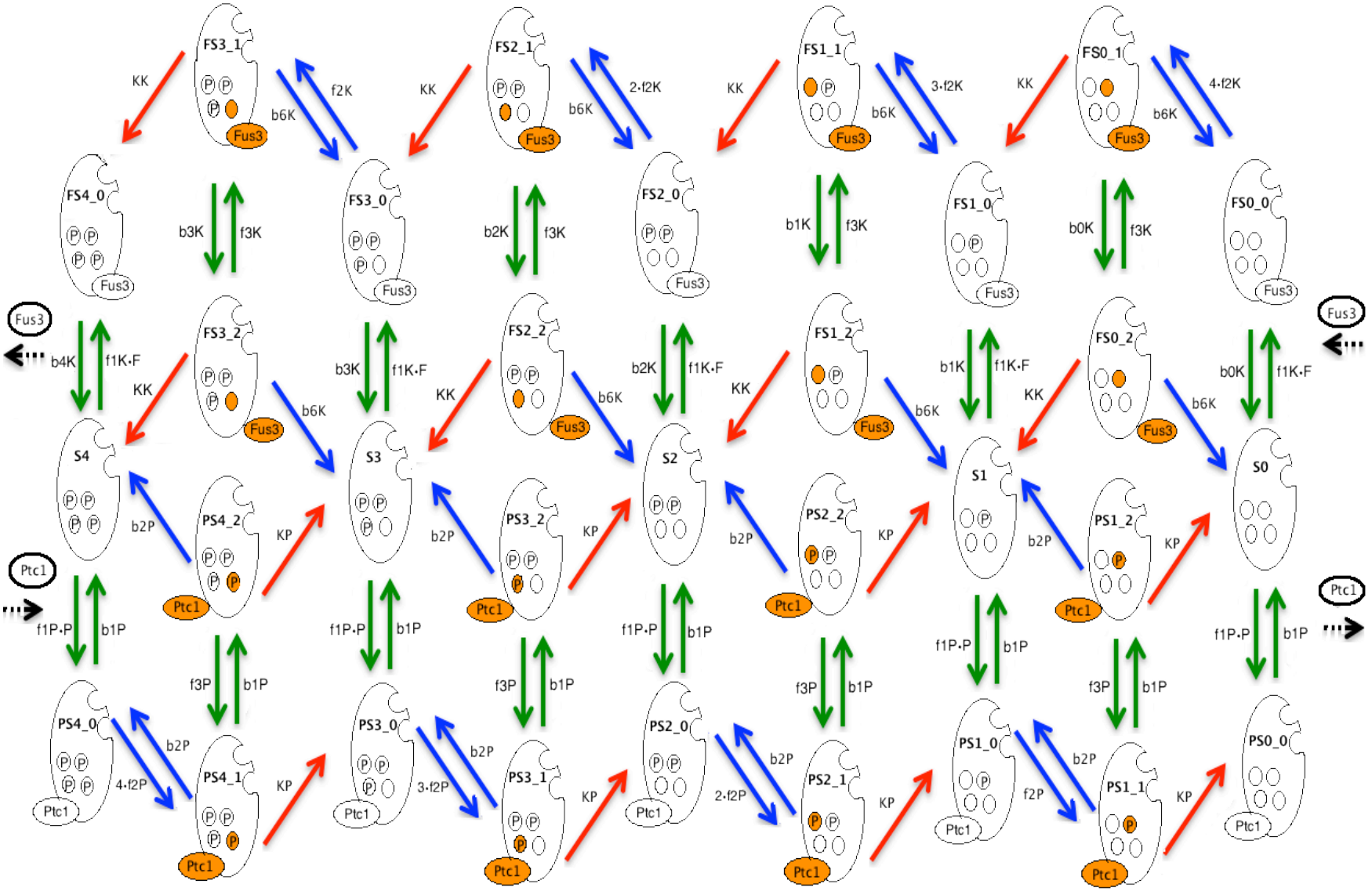
FS3_1
FS2_1
FS1_1
FS0_1
FS4_0
FS3_0
FS2_0
FS1_0
FS0_0
FS3_2
FS2_2
FS1_2
FS0_2
S4
S3
S2
S1
S0
PS4_2
PS3_2
PS2_2
PS1_2
PS4_0
PS3_0
PS2_0
PS1_0
PS0_0
PS4_1
PS3_1
PS2_1
PS1_1
Fus3
Ptc1
KK
KP
b6K
f2K
2·f2K
3·f2K
4·f2K
b3K
f3K
b2K
b1K
b0K
b4K
f1K·F
b2P
f1P·P
b1P
f3P
4·f2P
3·f2P
2·f2P
f2P

Figure 15. Modified model of Ste5, Fus3, and Ptc1. The modified model consists of different complexes: Sn is number (n) of phosphorylated phosphosites on Ste5, FSn_0 is number (n) of phosphorylated phosphosites on Ste5 while Fu3 is bound to the DM, FSn_1 is number (n) of phosphorylated phosphosites on Ste5 while Fus3 is bound to the DM and phosphorylate a new phosphosite, FSn_2 is number (n) of phosphorylated phosphosites on Ste5 while Fus3 phosphorylate a new phosphosite without being bound to the DM, Ste5-Ptc1 complexes have the same forms denoted by Ptc1_Ste5n_0, Ptc1_Ste5n_1, and Ptc1_Ste5n_2. The green arrows indicates that both Fus3 and Ptc1 must bind to the DM at Ste5, and the blue and red arrows indicates that Fus3 or Ptc1 are bound to the DM and are engaged in enzymatic reactions with phosphosites. Enzymes that are interacting with the phosphosites are highlighted in orange. From (Malleshaiah et al., 2010).

Reactions used to describe the system are listed in Appendix A, table A1. Reversible reactions denoted green and blue arrows can be seen in figure 15, but are not shown in the reactions set. The reaction set contains only reactions with one direction, describing every arrow in the modified model. All the reactions can be described by using ODEs that can be seen in the Appendix B, Equations. (22) – (30). In the ODEs the dot notation will be used, where $\dot{x}$ = dx/dt describes the concentration of each species x changing with time. The total reactions set consist of 76 reactions, described by nine differential equations. The total set of reactions has been used in the deterministic and stochastic simulation.

3.2 Assumptions related to the system

In the nature article by Malleshaiah et al. (Malleshaiah et al., 2010), concentrations of species and kinetic rates were given. The concentrations measured in M (moles per liter) were further calculated to molecule numbers to perform deterministic and stochastic simulations. In order to carry out the conversion from concentration to number per liter, volume of a yeast cell in liter must be known. The mean volume of a haploid yeast cell is given at 42 femtoliter (fL) (Jorgensen et al., 2002). 42 fL is 42 x 10^{-15} liter (L) and by multiplying the liter value with Avogadro´s constant (number of molecules in a mole) ≃6,023 x 10^{23}, it gives the number of molecules (Gillespie, 1977). The kinetic rates $f_1^{(K)}$ and $f_1^{(P)}$ have been converted from $nM^{-1}s^{-1}$ (nanomolar per second) to s^{-1} (molecules per second). The system has in total three species and 19 kinetic rates. Species and kinetic rates with their corresponding values have been used in the deterministic and stochastic simulations.

3.3 Deterministic analysis of the system

For the deterministic analysis, it was performed three simulations with different Ptc1 and Fus3 values. The Ptc1 values were 30, 500, and 1000 molecules and the Fus3 values were 100, 1188 and 5000 molecules. The number of Ste5 was increased from 100 to 1500 molecules. For the three simulations, rate constant values given in the nature article (Malleshaiah et al., 2010) were used (Appendix C, table c1 and c2). The three Fus3 values were used to analyze the mean of free and bound Ste5 molecules. The different free Ste5 complexes are denoted as S0, S1, S2, S3, and S4, figure 15. Mean of bound Ste5 in the three different Ste5-Fus3 complexes were calculated in order to evaluate the highest value of bound Ste5 in the system. The three different Ste5-Fus3 complexes were FSn_0, FSn_1, and FSn_2. Additionally, the values of the three different Ste5-Ptc1 complexes were calculated to evaluate the highest value of bound Ste5 in the system. The three different Ste5-Ptc1 complexes were PSn_0, PSn_1, and PSn_2.

3.3.1 Free Ste5 molecules

As mentioned above, the deterministic analysis of free Ste5 molecules was performed with Ptc1 values at 30, 500, and 1000 molecules and Fus3 values at 100, 1188 and 5000 molecules. The number of Ste5 molecules was increased from 100 to 1500 molecules. By increasing the number of Ste5 molecules at 30 Ptc1 molecules (Fig.16a), the mean of free Ste5 at 100 Fus3 molecules increased from zero to 1400 and remained zero at 5000 Fus3 molecules. The mean of Ste5 at 1188 Fus3 molecules increased from zero to about 30 due to an increase of Ste5 molecules from 1200 to 1500. Hence, by increasing the number of Fus3 molecules, there are less free Ste5 molecules in the system. By increasing the number of Ste5 molecules at 500 Ptc1 molecules (Fig.16b), the mean of Ste5 molecules at 1188 and 5000 remained zero. However, by increasing the number of Ste5 molecules from 550 to 1500 at 100 Fus3 molecules, the mean of free Ste5 increased from zero to 900 molecules. By increasing the number of Ste5 molecules at 1000 Ptc1 molecules (Fig.16c), the mean of free Ste5 molecules at 1188 and 5000 Fus3 molecules remained zero. At 100 Fus3 molecules, the mean of free Ste5 molecules increased from zero to 400 molecules due to an increase of Ste5 molecules from about 1050 to 1500. The mean of free Ste5 molecules for Ptc1 at 30, 500, and 1000 molecules and Fus3 at 100, 1188, and 500 molecules is given in Fig.16a-c, respectively.

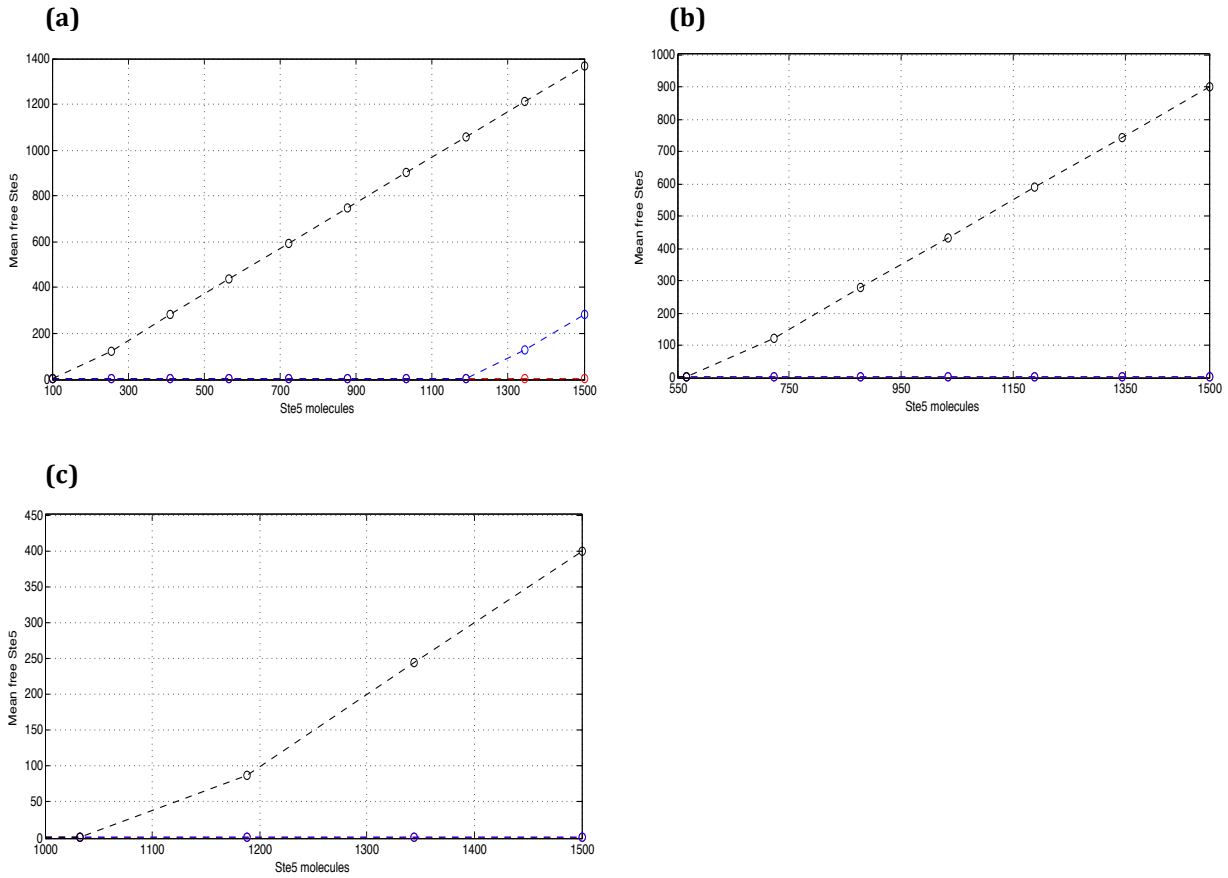

Figure 16. Mean of free Ste5 molecules. Calculated mean of free Ste5 molecules in the deterministic analysis. The Ptc1 values were 30, 500, and 1000 molecules and the Fus3 values were 100 (black), 1188 (blue), and 5000 (red) molecules. The number of Ste5 molecules was increased from 100 to 1500. **(a)** Ptc1 value at 30 with Fus3 values at 100, 1188, and 5000 molecules. By increasing the number of Ste5 molecules form 100 to 1500, the mean of free Ste5 at 5000 Fus3 molecules remained zero. At 100 Fus3 molecules, the mean of free Ste5 molecules increased from zero to 1400. The mean of Ste5 molecules at 1188 molecules increased from zero to about 300 due to an increase of Ste5 molecules from 1200 to 1500. **(b)** Ptc1 value at 500 with Fus3 values at 100, 1188, and 5000 Fus3 molecules. By increasing the number of Ste5 molecules from 100 to 1500, the mean of free Ste5 molecules at 1188 and 5000 remained zero. The mean of Ste5 molecules at 100 Fus3 molecules increased from zero to 900 due to an increase of Ste5 molecules from 500 to 1500. **(c)** Ptc1 value at 1000 with Fus3 at 100, 1188, and 5000 Fus3 molecules. By increasing the number of Ste5 molecules from 100 to 1500, the mean of free Ste5 molecules at 1188 and 5000 remained zero. The mean of Ste5 at 100 Fus3 molecules increased from zero to 400 due to an increase of Ste5 molecules from about 1050 to 1500.

3.3.2 Bound Ste5 molecules

The deterministic analysis of bound Ste5 molecules was performed with Ptc1 values at 30, 500, and 1000 molecules and Fus3 values at 100, 1188 and 5000 molecules. It was calculated the mean of bound Ste5 molecules in the three different Ste5-Fus3 complexes: FSn_0, FSn_1, and FSn_0. Additionally, it was calculated the mean of free Ste5 molecules. The number of Ste5 molecules was increased from 100 to 1500 molecules. By increasing the number of Ste5 molecules from 100 to 1500 at 30 Ptc1 and 5000 Fus3 molecules (17a), the mean of bound Ste5 molecules in the FSn_1 and FSn_2 complexes remained zero. The mean of bound Ste5 molecules in the FSn_0 complex increased from about 100 to 1500, and mean of free Ste5 decreased from 5000 to 3500 molecules. For 30 Ptc1 and 5000 Fus3 molecules (17b), the mean of bound Ste5 molecules in the FSn_2 complexes increased from zero to about 100 molecules and free Ste5 decreased from 5000 to 4000 molecules. The mean of bound Ste5 molecules in the FSn_1 complex increased from zero to about 100 after about 600 Ste5 molecules. In the FSn_0 complex, the mean of bound Ste5 molecules increased from zero to about 800 molecules from 600 to 1500 Ste5 molecules. By increasing the number of Ste5 molecules from 100 to 1500 at 1000 Ptc1 and 5000 Fus3 molecules (17c), the mean of bound Ste5 molecules in FSn_2 complex increased from zero to about 400 molecules and free ste5 decreased from 5000 to 4500. The mean of bound Ste5 molecules in FSn_0 and FSn_0 complex remained zero to about 1300 molecules, and then increased to about 100 molecules. By increasing the number of Ste5 molecules from 100 to 1300 at 30 Ptc1 and 1131 Fus3 molecules (17d), the mean of bound Ste5 molecules in the FSn_1 and FSn_2 complex remained at zero. The mean of bound Ste5 molecules in the FSn_0 complex increased from about 50 to about 1100 molecules, and free Ste5 decreased from about 1100 to zero. By increasing the number of Ste5 molecules from 100 to 1500 at 500 Ptc1 and 1131 Fus3 (17e), free Ste5 decreased from about 1100 to 200 molecules. Above 600 Ste5 molecules, the mean of bound Ste5 molecules in the FSn_0 complex increased from zero to about 800 molecules and from zero to 150 in the FSn_1 complex. From 100 to 700 Ste5 molecules, the mean of Ste5 molecules in the FSn_2 complex increased from about 50 to 150 molecules and by further increase of Ste5 molecules the mean decreased to 100 molecules. By increasing the number of Ste5 molecules from 100 to 1500 at 1000 Ptc1 and 1131 Fus3 molecules, free Ste5 decreased from about 1100 to 700 molecules. Both FSn_0 and FSn_1 complexes remained zero from 100 to 1350 Ste5 molecules and then increased to about 50 and 100 molecules. From 100 to 1350 Ste5 molecules, the mean of bound Ste5 molecules increased from about

50 to 400 molecules and then decreased to 300. By increasing the number of Ste5 molecules from 100 to 1500 at 30 Ptc1 and 100 Fus3 molecules (17g), the mean of bound Ste5 molecules in the FSn_1 complex increased from 10 to 40 molecules and from about 5 to 45 in the FSn_2 complex. From 100 to 250 Ste5 molecules, free Ste5 decreased from 30 to zero and the mean of bound Ste5 molecules in the FSn_0 complex increased from 55 to 85 molecules. The mean of bound Ste5 molecules in the FSn_0 complex decreased from 85 to 15 from 250 to 1500 Ste5 molecules. By increasing the number of Ste5 molecules from 100 to 700 at 500 Ptc1 and 100 Fus3 molecules (17h), the mean of bound Ste5 molecules in both FSn_0 and FSn_2 complexes remained zero. Free Ste5 decreased from about 85 to zero and the mean of bound Ste5 molecules in the FSn_2 complex increased from 15 to 100 molecules. By increasing the number of Ste5 molecules from 100 to 1200 at 1000 Ptc1 and 100 Fus3 molecules (17i), the mean of bound Ste5 molecules remained at zero. Free Ste5 decreased from 90 to zero and the mean of bound Ste5 molecules in the FSn_2 complex increased form 10 to 100 molecules. The distribution of bound Ste5 molecules in the three Ste5-Fus3 complexes and free Ste5 molecules are given in figure 17a-i, respectively.

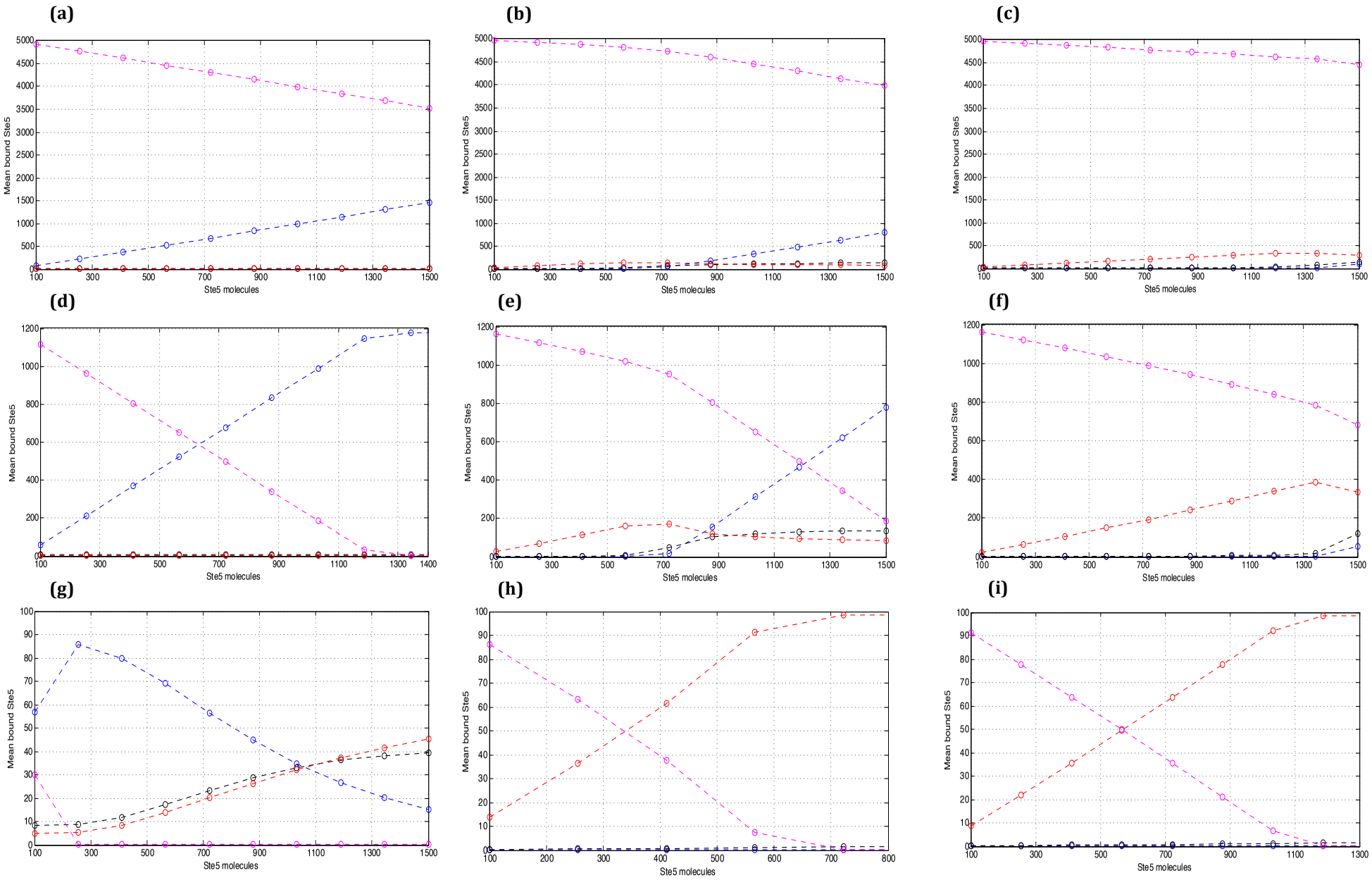
(a)
(b)
(c)
(d)
(e)
(f)
(g)
(h)
(i)
Mean bound Ste5
Ste5 molecules

Figure 17. Distribution of bound Ste5 molecules and free Ste5. Calculated mean of bound Ste5 molecules in the three different Ste5-Fus3 complexes and free Ste5 (magenta) molecules in the deterministic analysis. The Ste5-Fus3 complexes were FSn_0 (blue), FSn_1 (black) and FSn_2 (red). The Ptc1 values were 30, 500, and 1000 molecules and the Fus3 values were 100, 1188, and 5000 molecules. The number of Ste5 molecules was increased from 100 to 1500. **(a)** 30 Ptc1 and 5000 Fus3 molecules. By increasing the number of Ste5 molecules, free Ste5 molecules decreased and the mean of bound Ste5 molecules in the FSn_0 complex increased. **(b)** 500 Ptc1 and 5000 Fus3 molecules. By increasing the number of Ste5 molecules, free Ste5 molecules decreased and the mean of bound Ste5 molecules in the FSn_0 complex increased. Both FSn_1 and FSn_2 complexes had a slightly increase of bound Ste5 molecules. **(c)** 100 Ptc1 and 5000 Fus3 molecules. Due to an increase of Ste5 molecules, free Ste5 molecules decreased and the mean of bound Ste5 molecules in the FSn_2 complex increased. **(d)** 20 Ptc1 molecules and 1131 Fus3 molecules. By increasing the number of Ste5 molecules, free Ste5 decreased and the mean of bound Ste5 molecules in the FSn_0 complex increased. **(e)** 500 Ptc1 molecules and 1131 Fus3 molecules. Due to increased Ste5 molecules, free Ste5 molecules decreased and both FSn_0 and FSn_1 complexes increased. The mean of bound Ste5 in the FSn_2 complex increased from 100 to 700 Ste5 molecules and then decreased. **(f)** 1000 Ptc1 molecules and 1131 Fus3 molecules. Due to an increased number of Ste5 molecules, free Ste5 decreased and the mean of bound Ste5 molecules in the FSn_2 complex increased. **(g)** 30 Ptc1 and 100 Fus3 molecules. By increasing the number of Ste5 molecules, free Ste5 decreased and both FSn_1 and FSn_2 complexes increased. In the FSn_0 complex, the mean of Ste5 molecules increased from 100 to about 250 molecules and further decreased. **(h)** 500 Ptc1 molecules and 100 Fus3 molecules. By increasing the number of Ste5 molecules, free Ste5 molecules decreased and the mean of bound Ste5 molecules in the FSn_2 complex increased. **(i)** 1000 Ptc1 molecules and 100 Fus3 molecules. Due to increased Ste5 molecules, free Ste5 molecules decreased and the mean of bound Ste5 in the FSn_0 complex increased.

The deterministic analysis of bound Ste5 molecules was performed with Ptc1 values at 30, 500, and 1000 molecules and Fus3 values at 100, 1188 and 5000 molecules. It was calculated the mean of bound Ste5 molecules in the three different Ste5-Ptc1 complexes: PSn_0, PSn_1, and PSn_0. Additionally, it was calculated the mean of free Ste5 molecules. The number of Ste5 molecules was increased from 100 to 1500 molecules. By increasing the number of Ste5 molecules from 100 to 700 at 30 Ptc1 and 5000 Fus3 molecules (18a), free Ste5 decreased from about 6 to 1 molecules. The mean of bound Ste5 molecules in the PSn_2 complex increased form 23 to 28 molecules, remained zero in the PSn_0 complex and remained at about 2 molecules in the PSn_1 complex. By increasing the number of Ste5 molecules from 100 to 1200 at 500 Ptc1 and 1131 Fus3 molecules (18b), free Ste5 decreased from 425 to about 20 molecules and the mean of bound Ste5 molecules in the PSn_2 complex increased from about 70 to 470 molecules. In the PSn_1 complex, the mean of bound Ste5 molecules increased from about 10 to 20 molecules and decreased from about 20 to 10 in the PSn_0

complex. By increasing the number of Ste5 molecules form 100 to 1500 at 100 Ptc1 and 5000 Fus3 molecules (18c), free Ste5 molecules decreased from about 920 to 50 molecules and the mean of bound Ste5 molecules in the PSn_2 complex increased from 50 to 900 molecules. In PSn_1 complex, the mean of bound Ste5 molecules increased from 10 to 20 molecules and decreased from 10 to zero in the PSn_0 complex. By increasing the number of Ste5 molecules from 100 to 800 at 30 Ptc1 and 1131 Fus3 molecules (18d), free Ste5 molecules decreased from about 2 to zero and the mean of Ste5 molecules in the PSn_2 complex decreased from about 27 to 29 molecules. In the PSn_0 complex the mean of Ste5 molecules remained zero and remained at 2 in the PSn_1 complex. By increasing the number of Ste5 molecules from 100 to 1000 at 500 Ptc1 and 1131 Fus3 molecules (18e), free Ste5 molecules decreased from Bout 430 to zero molecules and the mean of bound Ste5 molecules in the PSn_2 complex increased from 60 to 470. In the PSn_1 complex the mean of Ste5 molecules increased from zero to 20 molecules and decreased from 20 to zero in the PSn_0 complex. By increasing the number of Ste5 molecules from 100 to 1500 at 1000 Ptc1 and 1131 Fus3 molecules (18f), free Ste5 molecules decreased from 920 to zero and the mean of bound Ste5 molecules in the PSn_2 complex increased from about 50 to 950 molecules. In the PSN_0 complex, the mean of Ste5 molecules increased from about 10 to 90 molecules and decreased to zero. The mean of Ste5 molecules in the PSn_1 complex increased from zero to 50 molecules. By increasing the number of Ste5 molecules from 100 to 1500 at 30 Ptc1 and 100 Fus3 molecules (18g), both free Ste5 and the mean of bound Ste5 molecules in the PSn_0 complex remained at zero. In the PSn_1 complex, the mean of bound Ste5 molecules remained at 2 molecules and remained at 28 in the PSn_2 complex. By increasing the number of Ste5 molecules from 100 to 800 molecules at 500 Ptc1 and 100 Fus3 molecules (18h), free Ste5 molecules decreased from about 420 to zero and the mean of bound Ste5 molecules in the PSn_1 complex increased from zero to 10 molecules. In the PSn_0 complex, the mean of bound Ste5 molecules increased from 50 to 270 molecules and increased from 30 to 220 molecules in the PSn_2 complex. By increasing the number of Ste5 from 100 to 1300 molecules at 1000 Ptc1 and 100 Fus3 molecules (18i), free Ste5 molecules decreased from 900 to zero molecules and the mean of bound Ste5 molecules in the PSn_1 complex remained at zero. In the PSn_0 complex, the mean of bound Ste5 molecules increased from about 80 to 780 molecules and increased from about 20 to 210 in the PSn_2 complex. The distribution of bound Ste5 molecules in the three Ste5_ptc1 complexes and free Ste5 molecules can be seen in figure 18a-i, respectively.

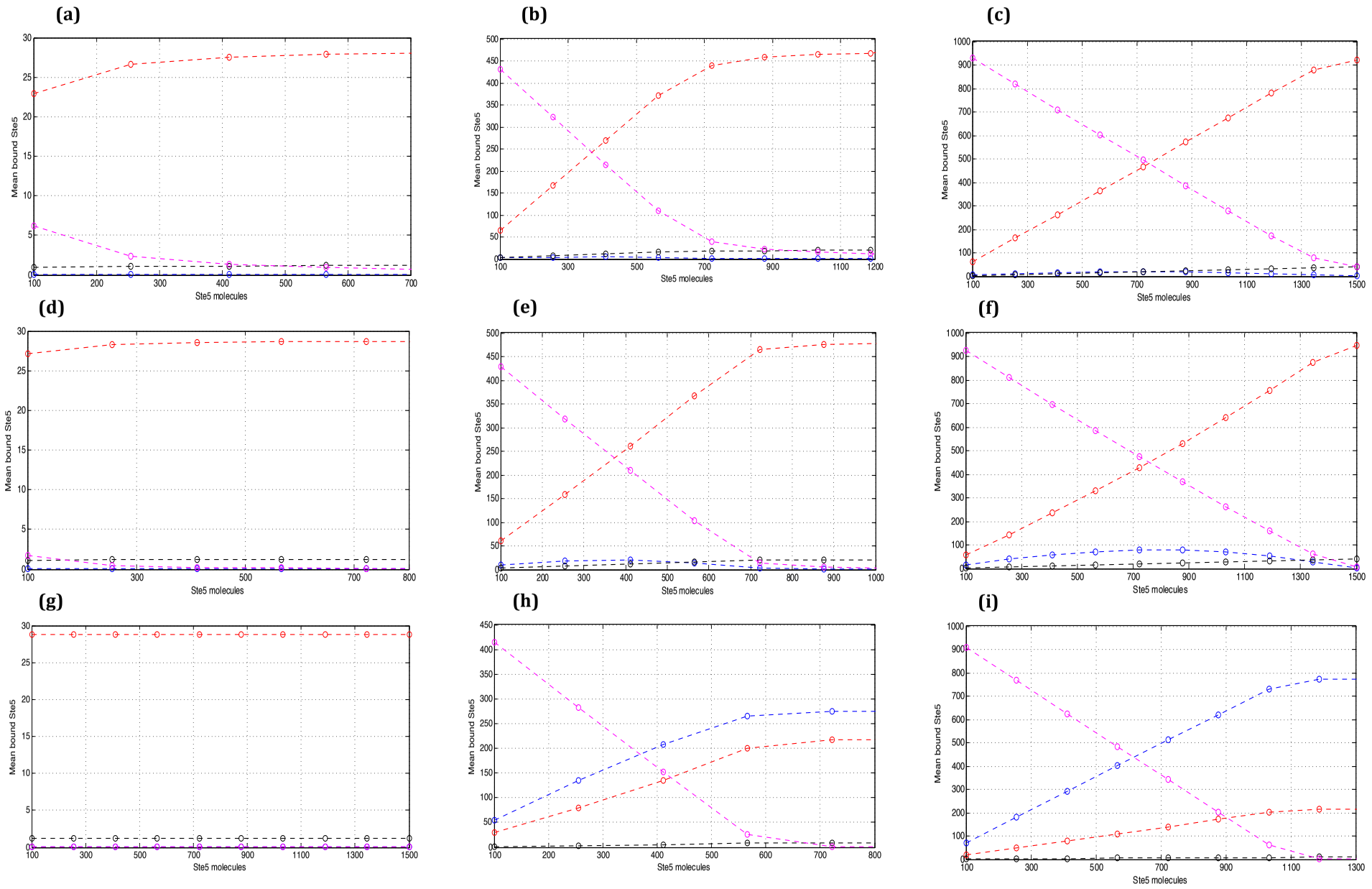
(a)
(b)
(c)
(d)
(e)
(f)
(g)
(h)
(i)
Mean bound Ste5
Ste5 molecules

Figure 18. Distribution of bound Ste5 molecules and free Ste5. Calculated mean of bound Ste5 molecules in the three different Ste5-Ptc1 complexes and free Ste5 (magenta) molecules in the deterministic analysis. The Ste5-Ptc1 complexes were PSn_0 (blue), PSn_1 (black) and PSn_2 (red). The Ptc1 values were 30, 500, and 1000 molecules and the Fus3 values were 100, 1188, and 5000 molecules. The number of Ste5 molecules was increased from 100 to 1500. **(a)** 30 Ptc1 and 5000 Fus3 molecules. By increasing the number of Ste5 molecules from 100 to 700, free Ste5 decreased and the mean of bound Ste5 in the PSn_2 complex increased. The mean of bound Ste5 was constant at 2 molecules in the PSn_1 complex and constant at zero in the PSn_0 complex. **(b)** 500 Ptc1 and 5000 Fus3 molecules. By increasing the number of bound Ste5 molecules from 100 to 1200 molecules, free Ste5 molecules increased and the mean of bound Ste5 molecules in both the PSn_1 and PSn_2 complexes increased. In the PSn_0 complex, the mean of bound Ste5 molecules remained at zero. **(c)** 1000 Ptc1 and 5000 Fus3 molecules. By increasing the number of Ste5 molecules from 100 to 1500, free Ste5 decreased and the mean of bound Ste5 molecules in the PSn_1 and PSn_2 complexes increased. In PSn_0 complex, the mean of bound Ste5 increased from 100 to about 900 molecules and the decreased. **(d)** 30 Ptc1 molecules and 1131 Fus3 molecules. By increasing the number of Ste5 molecules from 100 to 800, free Ste5 decreased and the mean of bound Ste5 molecules in the PSn_2 complex increased. The mean of bound Ste5 molecules remain constant at about 2 molecules in the PSn_1 complex and zero in the PSn_0 complex. **(e)** 500 Ptc1 and 1131 Fus3 molecules. By increasing the number of Ste5 molecules from 100 to 1000, free Ste5 decreased and the mean of bound Ste5 molecules in both PSn_1 and PSn_2 complexes increased. The mean of Ste5 molecules in the PSn_0 complex increased from 100 to about 400 Ste5 molecules and then decreased. **(f)** 1000 Ptc1 molecules and 1131 Fus3 molecules. By increasing the number of Ste5 molecules from 100 to 1500, free Ste5 decreased and the mean of bound Ste5 molecules in both PSn_1 and PSn_2 complexes increased. The mean of bound Ste5 molecules in the PSn_0 complex increase from 100 to about 800 Ste5 molecules and then decreased. **(g)** 30 Ptc1 and 100 Fus3 molecules. By increasing the number of Ste5 molecules from 100 to 1500, both free Ste5 molecules and the mean of bound Ste5 molecules in the PSn_0 complex remained at zero. The mean of bound Ste5 molecules in the PSn_1 complex remained at 2 molecules and it remained at 28 in the PSn_2 complex. (h) 500 Ptc1 molecules and 100 Fus3 molecules. By increasing the number of Ste5 molecules from 100 to 800, free Ste5 decreased and the mean of bound Ste5 molecules in PSn_0, PSn_1, and PSn_2 complexes increased. **(i)** 1000 Ptc1 and 100 Fus3 molecules. By increasing the number of Ste5 molecules from 100 to 1300, free Ste5 decreased. The mean of bound Ste5 molecules in PSn_0, PSn_1, and PSN_2 complexes increased.

3.3.3 Bound Ste5 molecules in single complexes

After measuring the mean for the three different Ste5-Fus3 and Ste5-Ptc1 complexes above with different Ptc1 and Fus3 values, most bound Ste5 molecules are located in the FSn_0 complex. In the deterministic analysis, the mean of bound Ste5 molecules in single complexes were calculated in order to evaluate the distribution of bound Ste5 molecules. The calculations were performed at 30 Ptc1 and 100 and 5000 Fus3 molecules. The number of Ste5 molecules increased from 100 to 1500. At 30 Ptc1 and 100 Fus3 molecules, the highest

mean of bound Ste5 molecules was located in the FS4_0 complex at 48 molecules, highlighted in yellow. At 30 Ptc1 and 5000 Fus3 molecules, the highest mean of bound Ste5 molecules was located in the FS4_0 complex at 758 molecules, highlighted in yellow. Calculated mean of bound Ste5 molecules in single complexes for deterministic analysis can be seen in table 2.

Table 2. Calculated mean of bound Ste5 molecules in single complexes. Calculated mean of bound Ste5 molecules in single complexes in the deterministic analysis. The number of Ste5 molecules increased from 100 to 1500. The calculations were performed at 30 Ptc1 and 100 and 5000 Fus3 molecules. At 30 Ptc1 and 100 Fus3 molecules, the highest mean of bound Ste5 molecules was located in the FS4_0 complex at 48 molecules. At 30 Ptc1 and 5000 Fus3 molecules, the highest mean of bound Ste5 molecules was located in the FS4_0 complex at 758 molecules. The two highest values of bound Ste5 molecules are highlight in yellow.

Complex	**Fus3=100 (mean)**	**Fus3=5000 (mean)**	**Complex**	**Fus3=100 (mean)**	**Fus3=5000 (mean)**	**Complex**	**Fus3=100 (mean)**	**Fus3=5000 (mean)**
FS4_0	48	758	FS3_1	12	8	FS3_2	6	6
FS3_0	1	0	FS2_1	8	0	FS2_2	7	7
FS2_0	0	0	FS1_1	5	0	FS1_2	0	0
FS1_0	0	0	FS0_1	0	0	FS0_2	3	3
FS0_0	0	0						
PS4_0	0	0	PS3_1	1	1	PS3_2	13	26
PS3_0	0	0	PS2_1	0	0	PS2_2	5	2
PS2_0	0	0	PS1_1	0	0	PS1_2	5	0
PS1_0	0	0	PS0_1	0	0	PS0_2	6	0
PS0_0	0	0						

3.4 Stochastic analysis of the system

The system can be explored further by exposing it to stochastic fluctuations. By this, it is possible to verify the bistable regions and the stability of stable steady states. It was performed three simulations due to different Ptc1 values. The Ptc1 values were 30, 500, and 1000 molecules. The number of Ste5 molecules was increased from 100 to 1500, and the values of Fus3 were 100, 1131, and 5000 molecules. The three Fus3 values were used to analyze the mean of free and bound Ste5 molecules. The different free Ste5 complexes are denoted as S0, S1, S2, S3, and S4, figure 15. Mean of bound Ste5 in the three different Ste5-

Fus3 complexes were calculated in order to evaluate the highest value of bound Ste5 in the system. The three different Ste5-Fus3 complexes were FSn_0, FSn_1, and FSn_2. Additionally, the values of the three different Ste5-Ptc1 complexes were calculated to evaluate the highest value of bound Ste5 in the system. The three different Ste5-Ptc1 complexes were PSn_0, PSn_1, and PSn_2. During the three simulations, the kinetic rate values were constant. Additionally, the rate constant $f_l^{(K)}$ and $f_l^{(P)}$ were changed. In the nature article, the value of $f_l^{(K)}$ at 480 molecules per second, and the value of $f_l^{(P)}$ at 7400 molecules per second were given. Two simulations were performed with a decreased and increased $f_l^{(K)}$ value at 100 and 1000 molecules per second, and two simulations with a decreased and increased $f_l^{(P)}$ value at 100 and 15000 molecules per second. Additionally, the standard deviation, Cov and fano factor were measured at 100 Fus3 and 30 Ptc1 molecules.

3.4.1 Free Ste5 molecules

As mentioned above, the stochastic analysis of free Ste5 molecules was performed with Ptc1 values at 30, 500, and 1000 molecules and Fus3 values at 100, 1131 and 5000 molecules. The number of Ste5 molecules was increased from 100 to 1500 molecules. Due to similar values of free Ste5 molecules in the stochastic and deterministic analysis, the distribution of free Ste5 molecules was not plotted. The plot of free Ste5 molecules can be seen in Fig.16a-c.

3.4.2 Bound Ste5 molecules

The stochastic analysis of bound Ste5 molecules was performed with Ptc1 values at 30, 500, and 1000 molecules and Fus3 values at 100, 1131 and 5000 molecules. It was calculated the mean of bound Ste5 molecules in the three different Ste5-Fus3 complexes: FSn_0, FSn_1, and FSn_0. Additionally, it was calculated the mean of free Ste5 molecules. The number of Ste5 molecules was increased from 100 to 1500 molecules. By increasing the number of Ste5 molecules from 100 to 1500 at 30 Ptc1 and 5000 Fus3 molecules (19a), free Ste5 decreased from 4900 to 3500 molecules, and the mean of bound Ste5 molecules in the FSn_0 complex increased from 100 to 1500 molecules. In both FSn_1 and FSn_2 complexes, the mean of bound Ste5 molecules remained at zero. By increasing the number of Ste5 molecules from 100 to 1500 at 500 Ptc1 and 5000 Fus3 molecules (19b), free Ste5 molecules decreased from 5000 to 4000 molecules and the mean of bound Ste5 molecules in the FSn_0 complex

increased from zero to about 700 molecules. In the FSn_1 complex, the mean of bound St5e molecules increased form zero to about 200 molecules at 600 Ste5 molecules and then remained constant. The mean of bound Ste5 molecules in the FSn_2 complex remained constant at about 200 molecules. By increasing the number of Ste5 molecules from 100 to 1500 at 1000 Ptc1 and 5000 Fus3 (19c), free Ste5 decreased form 500 to 4500 Ste5 molecules. The mean of bound Ste5 molecules in the FSn_2 complex increased from 100 to 400 Ste5 molecules. In Both FSn_0 and FSn_1 complexes the mean of bound Ste5 molecules increased from zero to about 500 Ste5 molecules from 1300 Ste5 molecules. By increasing the number of Ste5 molecules at 30 Ptc1 and 1131 Fus3 molecules (19d), free Ste5 decreased from about 1100 to zero and the mean of bound Ste5 molecules in both FSn_1 and FSN_2 remained at zero. In the FSn_0 complex, the mean of bound Ste5 molecules increased from about 50 to 1100 Ste5 molecules. By increasing the number of Ste5 molecules from 100 to 1500 at 500 Ptc1 and 1131 Fus3 molecules (19e), free Ste5 molecules decreased from about 1100 to 100 and the mean of bound Ste5 molecules in the FSn_0 complex increased from zero to 800 after 700 Ste5 molecules. In the FSn_1 complex, the mean of bound Ste5 molecules increased from zero to 100 molecules from 700 Ste5 molecules and remained constant. The mean of bound Ste5 molecules in the FSn_2 complex increased from zero to 200 and decreased to 100 Ste5 molecules after 700 Ste5 molecules. By increasing the number of Ste5 molecules from 100 to 1500 Ste5 molecules at 1000 Ptc1 and 1131 Fus3 molecules (19f), free Ste5 molecules decreased from about 1100 to 600 molecules and the mean of bound Ste5 molecules in the FSn_2 complex increased from about 20 to 400 molecules and decreased to 300 after 1400 Ste5 molecules. In the FSn_1 complex, the mean of bound Ste5 molecules increased after 1400 Ste5 molecules to 100 molecules and to 50 molecules in the FSn_0 complex. By increasing the number of Ste5 molecules from 100 to 1500 at 30 Ptc1 and 100 Fus3 molecules (19g), free Ste5 molecules increased from 30 to zero and remained zero after 200 Ste5 molecules. In both FSn_1 and FSn_2 complexes, the man of bound Ste5 molecules increased from about 5 to 25 molecules. The mean of bound Ste5 molecules in the FSn_0 complex increased from 55 to 85 molecules and decreased to 55 molecules after 200 Ste5 molecules. By increasing the number of Ste5 molecules from 100 to 700 at 500 Ptc1 and 100 Fus3 molecules (19h), free Ste5 molecules decreased from 85 to zero and the mean of bound Ste5 molecules in the FSn_2 complex increased from about 15 to 98 Ste5 molecules. The mean of bound Ste5 molecules in the FSn_1 complex had a slightly increase from zero to 3 molecules after 400 Ste5 molecules and it remained zero in the FSn_0 complex. By increasing the number of Ste5 molecules from 100 to 1200 at 1000 Ptc1 and 100 Fus3

molecules (19i), free Ste5 decreased form 90 to zero molecules and the mean of bound Ste5 molecules in the FSn_2 complex increased from 10 to 98 molecules. The mean of bound Ste5 molecules in the FSn_1 complex had a slightly increase from zero to 3 molecules after 400 Ste5 molecules and it remained zero in the FSn_0 complex. The distribution of bound Ste5 molecules in the three Ste5-Fus3 complexes and free Ste5 can be seen in Fig.19a-I, respectively.

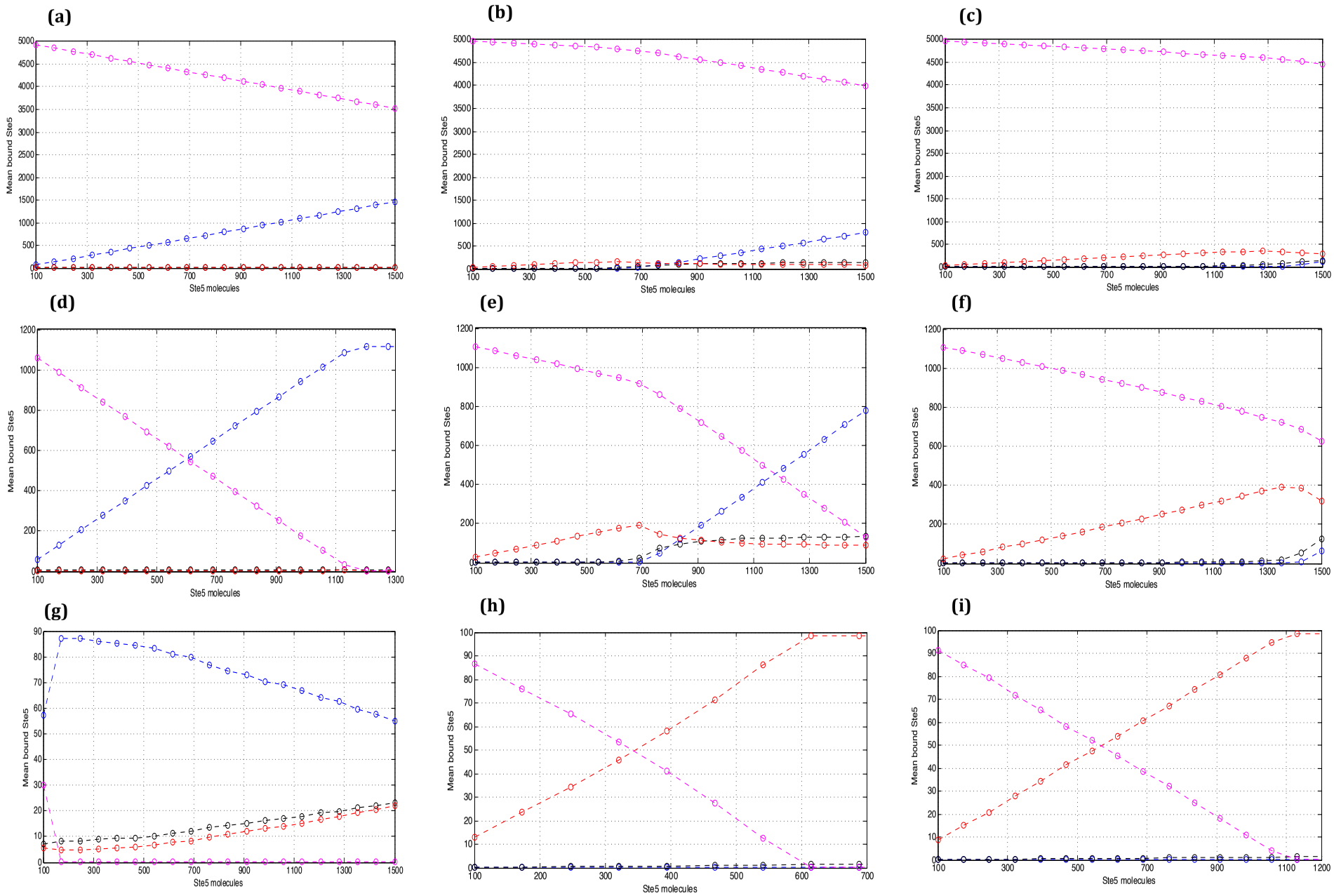
(a)
(b)
(c)
(d)
(e)
(f)
(g)
(h)
(i)
Mean bound Ste5
Ste5 molecules

Figure 19. Distribution of bound Ste5 molecules and free Ste5. Calculated mean of bound Ste5 molecules in the three different Ste5-Fus3 complexes and free Ste5 (magenta) molecules in the stochastic analysis. The Ste5-Fus3 complexes were FSn_0 (blue), FSn_1 (black) and FSn_2 (red). The Ptc1 values were 30, 500, and 1000 molecules and the Fus3 values were 100, 1131, and 5000 molecules. The number of Ste5 molecules was increased from 100 to 1500. (a) 30 Ptc1 and 5000 Fus3 molecules. By increasing the number of Ste5 molecules, free Ste5 decreased and the mean of bound Ste5 in the FSn_0 complex decreases. In both FSn_1 and FSn_2 complex, the mean of bound Ste5 remained zero. (b) 500 Ptc1 and 5000 Ste5 molecules. By increasing the number of Ste5 molecules, free Ste5 decreased, the mean of bound Ste5 molecules in both FSn_0 and FSn_1 complexes increased and remained constant in the FSN_2 complex. (c) 1000 Ptc1 and 5000 Ste5 molecules. By increasing the number of Ste5 molecules, free Ste5 decreased and the mean of bound Ste5 in FSn_0, FSn_1, and FSn_2 complex increased. (d) 30 Ptc1 and 1131 Fus3 molecules. By increasing the number of Ste5 molecules, free Ste5 molecules decreased and the mean of bound Ste5 molecules in the FSn_0 complex increased. In both FSn_1 and FSn_2 complexes, the mean of bound Ste5 molecules remained at zero. (e) 500 Ptc1 and 1131 Fus3 molecules. By increasing the number of Ste5 molecules, free Ste5 decreased ant the mean of bound Ste5 molecules in the FSn_0 complex increased. In the FSn_2 complex, the mean of bound Ste5 molecules increased to 700 Ste5 molecules and then remained constant. The mean of bound Ste5 molecules in the FSn_1 complex increased to 900+ Ste5 molecules and then remained constant. (f) 1000 Ptc1 and 1131 Fus3 molecules. By increasing the number of Ste5 molecules, free Ste5 decreased and the mean of bound Ste5 molecules in the FSn_0, FSn_1, and FSn_2 complexes increased. (g) 30 Ptc1 molecules and 100 Fus3 molecules. By increasing the number of Ste5 molecules, free Ste5 and the mean of bound Ste5 molecules in the FSn_0 complex decreased. The mean of bound Ste5 molecules sin both FSn_1 and FSn_2 complexes increased. (h) 500 Ptc1 and 100 Ste5 molecules. By increasing the number of Ste5 molecules, free Ste5 molecules decreased and the mean of bound Ste5 in the FSn_2 complex increased. In both FSn_0 and FSn_1 complexes, the mean of bound Ste5 molecules remained at zero. (i) 1000 Ptc1 and 100 FUs3 molecules. By increasing the number of Ste5 molecules, free Ste5 decreased and the mean of bound Ste5 molecules in the FSn_2 complex increased. In both the FSn_0 and FSn_1 complexes, the mean of bound Ste5 molecules remained at zero.

The stochastic analysis of bound Ste5 molecules was performed with Ptc1 values at 30, 500, and 1000 molecules and Fus3 values at 100, 1131 and 5000 molecules. It was calculated the mean of bound Ste5 molecules in the three different Ste5-Ptc1 complexes: PSn_0, PSn_1, and PSn_0. Additionally, it was calculated the mean of free Ste5 molecules. The number of Ste5 molecules was increased from 100 to 1500 molecules. Due to similar values of bound Ste5 and free Ste5 molecules in the deterministic and stochastic analysis, the distribution of bound Ste5 molecules was not plotted. However, the plot for bound Ste5 and free Ste5 molecules in the deterministic analysis can be seen in figure 18a-i, respectively.

3.5 Bound Ste5 molecules in single complexes

After measuring the mean for the three different Ste5-Fus3 and Ste5-Ptc1 complexes above with different Ptc1 and Fus3 values, most bound Ste5 molecules are located in the FSn_0 complex. In the stochastic analysis, the mean of bound Ste5 molecules in single complexes were calculated in order to evaluate the distribution of bound Ste5 molecules. The calculations were performed at 30 Ptc1 and 100 and 5000 Fus3 molecules. The number of Ste5 molecules increased from 100 to 1500. At 30 Ptc1 and 100 Fus3 molecules, the highest mean of bound Ste5 molecules was located in the FS4_0 complex at 72 molecules, highlighted in yellow. At 30 Ptc1 and 5000 Fus3 molecules, the highest mean of bound Ste5 molecules was located in the FS4_0 complex at 757 molecules, highlighted in yellow. Calculated mean of bound Ste5 molecules in single complexes for stochastic analysis can be seen in table 3.

Table 3. Calculated mean of bound Ste5 molecules in single complexes. Calculated mean of bound Ste5 molecules in single complexes in the stochastic analysis. The number of Ste5 molecules increased from 100 to 1500. The calculations were performed at 30 Ptc1 and 100 and 5000 Fus3 molecules. At 30 Ptc1 and 100 Fus3 molecules, the highest mean of bound Ste5 molecules was located in the FS4_0 complex at 72 molecules. At 30 Ptc1 and 5000 Fus3 molecules, the highest mean of bound Ste5 molecules was located in the FS4_0 complex at 757 molecules. The two highest values of bound Ste5 molecules are highlight in yellow.

Complex	**Fus3=100 (mean)**	**Fus3=5000 (mean)**	**Complex**	**Fus3=100 (mean)**	**Fus3=5000 (mean)**	**Complex**	**Fus3=100 (mean)**	**Fus3=5000 (mean)**
FS4_0	72	757	FS3_1	9	8	FS3_2	5	4
FS3_0	0	0	FS2_1	4	0	FS2_2	3	0
FS2_0	0	0	FS1_1	2	0	FS1_2	3	0
FS1_0	0	0	FS0_1	0	0	FS0_2	1	0
FS0_0	0	0						
PS4_0	0	0	PS3_1	1	1	PS3_2	20	26
PS3_0	0	0	PS2_1	0	0	PS2_2	1	2
PS2_0	0	0	PS1_1	0	0	PS1_2	2	0
PS1_0	0	0	PS0_1	0	0	PS0_2	2	0
PS0_0	0	0						

3.6 Standard deviation

The standard deviation in the three different Ste5-Fus3 complexes for a Ptc1 value at 30 and Fus3 values at 100 and 5000 molecules were performed. The number of Ste5 was increased from 100 to 1500 molecules. By increasing the number of Ste5 molecules at 30 Ptc1 and 100 Fus3 molecules (20a), the standard deviation of bound Ste5 molecules increased. The standard deviation of the FSn_0 complex increased from about 5 to 26, from 5 to 14 in the FSn_1 complex, and from 5 to 18 in the FSn_2 complex. By increasing the number of Ste5 molecules from 100 to 1500 at 30 Ptc1 and 5000 Fus3 molecules (20b), the standard deviation in the FSn_0 complex varied from about 1,7 to 4,6, from 3,3 to 3,8 in the FSn_1 complex, and from 2,6 to 3,3 in the FSn_2 complex. The standard deviation of Ste5 in the three different Ste5-Fus3 complexes at 30 Ptc1 and 100 and 500 Fus3 molecules can be seen in figure 20a and b, respectively.

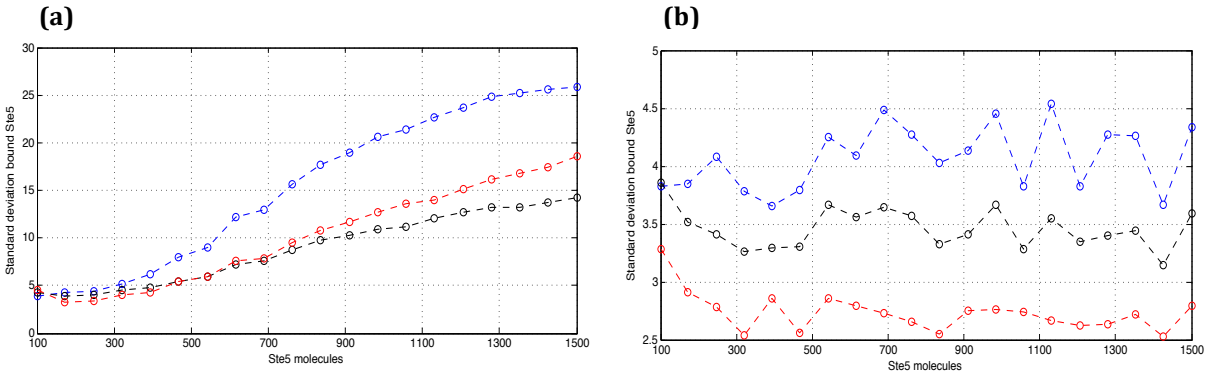

Figure 20. Standard deviation of bound Ste5 molecules in the Ste5-Fus3 complexes. Standard deviation of bound Ste5 molecules in FSn_0 (blue), FSn_1 (black), and FSn_2 (red) complexes at 30 Ptc1 and 100 and 5000 Fus3 molecules. The number of Ste5 increased from 100 to 1500 molecules. **(a)** 30 Ptc1 and 100 Fus3 molecules. By increasing the number of Ste5 molecules, the standard deviation in all three Ste5-Fus3 complexes increased. **(b)** 30 Ptc1 and 5000 Fus3 molecules. By increasing the number of Ste5 molecules, the standard deviation in all the three Ste5-Fus3 complexes varied.

The standard deviation of bound Ste5 molecules in the three different Ste5-Ptc1 complexes for a Ptc1 value at 30 and Fus3 values at 100 and 5000 molecules were performed. The number of Ste5 was increased from 100 to 1500 molecules. By increasing the number of Ste5 molecules from 100 to 200 at 30 Ptc1 and 100 Fus3 molecules (21a), the standard deviation bound Ste5 molecules in the FSn_2 complex decreased from about 8 to 4,5. Due to increased

number of Ste5 molecules from 200 to 1500, the standard deviation of bound Ste5 molecules increased from about 4,5 to 16. The standard deviation of bound Ste5 molecules in the FSn_0 complex remained constant at 2 and at 0,5 in the FSn_2 complex. By increasing the number of Ste5 molecules from 100 to 1500 molecules at 30 Ptc1 and 5000 Fus3 molecules (21b), the standard deviation of bound Ste5 molecules in the FSn_1 complex remained constant at 1,5 and at 0,5 in the FSn_0 complex. The standard deviation of bound Ste5 molecules in the FSn_2 complex decreased from about 5,5 to 2,5. The standard deviation of bound Ste5 molecules at 30 Ptc1 and 100 and 5000 Fus3 molecules can be seen in figure 21a-b, respectively.

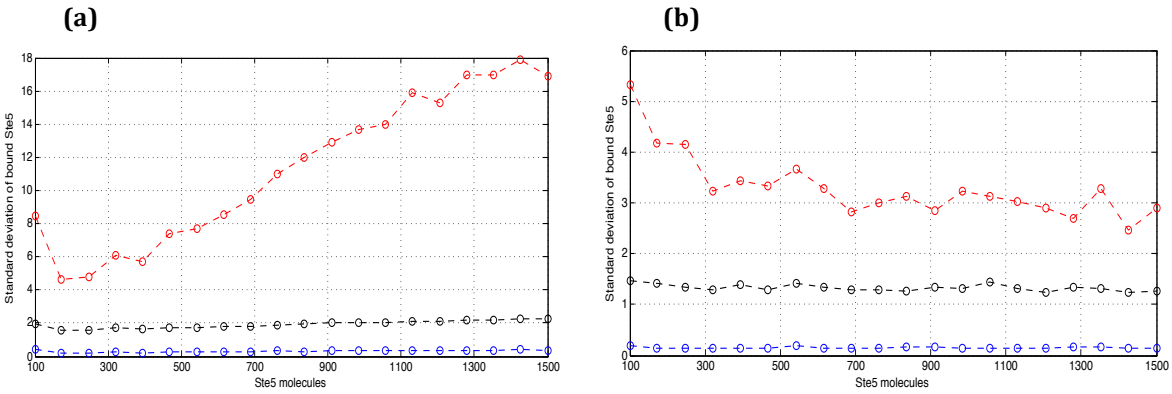

Figure 21. Standard deviation of bound Ste5 molecules in the Ste5-Ptc1 complexes. Standard deviation of bound Ste5 molecules in PSn_0 (blue), PSn_1 (black), and PSn_2 (red) complexes at 30 Ptc1 and 100 and 5000 Fus3 molecules. The number of Ste5 increased from 100 to 1500 molecules. **(a)** 30 Ptc1 and 100 Fus3 molecules. By increasing the number of Ste5 molecules, the standard deviation of bound Ste5 molecules in the PSn_2 complex increased. The standard deviation of bound Ste5 molecules in the PSn_1 complex remained constant at about 2 and at 0,5 in the FSn_0 complex. **(b)** 30 Ptc1 and 5000 Fus3 molecules. By increasing the number of Ste5 molecules, the standard deviation of bound Ste5 molecules in the PSn_2 complex decreased and remained constant in both PSn_0 and PSn_1 complex. .

3.7 Coefficient of variation

The coefficient of variation (CoV) in the three different Ste5-Fus3 complexes for a Ptc1 value at 30 and Fus3 values at 100 and 5000 molecules were performed. The number of Ste5 was increased from 100 to 1500 molecules. By increasing the number of Ste5 molecules from 100 to 1500 at 30 Ptc1 and 100 Fus3 molecules (22a), the CoV of bound Ste5 molecules in the FSn_0 complex increased from about 0,05 to 0,5. The CoV of bound Ste5 molecules in the

FSn_1 complex varied from 0,45 to 0,65, and from about 0,7 to 1 in the FSn_2 complex. By increasing the number of Ste5 molecules from 100 to 1500 at 30 Ptc1 and 5000 Fus3 molecules (22b), the CoV of bound Ste5 molecules in FSn_0 complex decreased from 0,05 to zero, from 0,6 to 0,4 in the FSn_1 complex, and from 0,85 to about 0,6 in the FSn_2 complex. The CoV of bound Ste5 molecules in the three different Ste5-Fus3 molecules at 30 Ptc1 and 100 and 5000 Fus3 molecules can be seen in figure 22a-b, respectively.

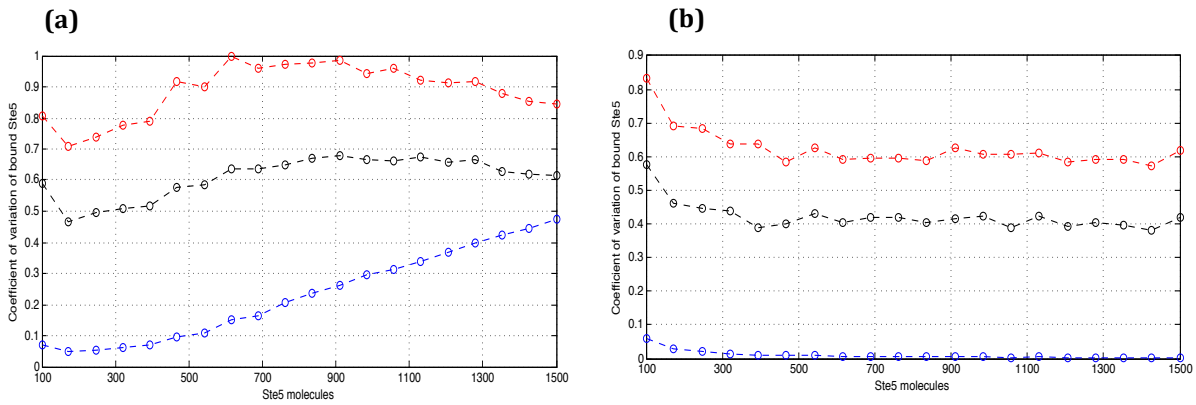

Figure 22. Coefficient of variation of bound Ste5 molecules in the Ste5-Fus3 complexes. CoV of bound Ste5 molecules in FSn_0 (blue), FSn_1 (black), and FSn_2 (red) complexes at 30 Ptc1 and 100 and 5000 Fus3 molecules. The number of Ste5 increased from 100 to 1500 molecules. **(a)** 30 Ptc1 and 100 Fus3 molecules. By increasing the number of Ste5 molecules, the CoV of bound Ste5 molecules in the FSn_0 complex increased, varied from 0,45 to 0,7 in the FSn_1 complex, and varied from 0,7 to 1 in the FSn_2 complex. (b) 30 Ptc1 and 5000 Fus3 molecules. By increasing the number of Ste5 molecules, the CoV of bound Ste5 molecules in all the three Ste5-Fus3 complexes decreased and remained constant.

The CoV of bound Ste5 molecules in the three different Ste5-Ptc1 complexes for a Ptc1 value at 30 and Fus3 values at 100 and 5000 molecules were performed. The number of Ste5 was increased from 100 to 1500 molecules. By increasing the number of Ste5 molecules from 100 to 1500 at 30 Ptc1 and 100 Fus3 molecules (23a), the CoV of bound Ste5 molecules in the PSn_0 complex decreased from 5,5 to 1. The CoV of bound Ste5 molecules in the PSn_1 complex decreased from about 1,5 to 1,3 from 100 to 200 Ste5 molecules and further increased to 1,8. The CoV of bound Ste5 molecules in the PSn_2 complex decreased from about 0,5 to 0,2 from 100 to 200 Ste5 molecules and further increased to 0,8. By increasing the number of Ste5 molecules at 30 Ptc1 and 5000 Fus3 molecules (23b), the CoV of bound Ste5 molecules in the PSn_1 remained constant at about 1,5 and remained constant at about

0,2 in and PSn_2 complexes. The CoV of bound Ste5 molecules at 30 Ptc1 and 100 and 5000 Fus3 molecules in the three different Ste5-Ptc1 complexes can be seen in figure 23a-b, respectively.

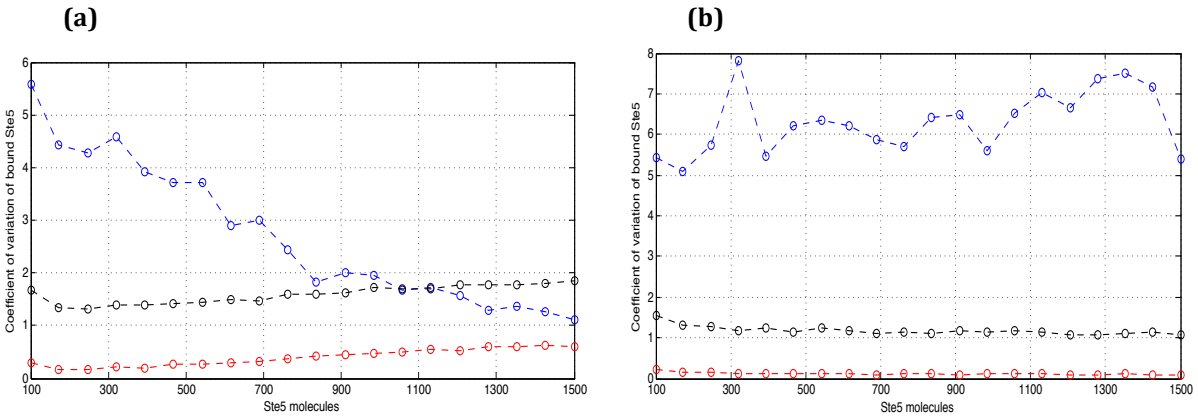

Figure 23. Coefficient of variation of bound Ste5 molecules in the Ste5-Ptc1 complexes. CoV of bound Ste5 molecules in PSn_0 (blue), PSn_1 (black), and PSn_2 (red) complexes at 30 Ptc1 and 100 and 5000 Fus3 molecules. The number of Ste5 increased from 100 to 1500 molecules. **(a)** 30 Ptc1 and 100 Fus3 molecules. By increasing the number of Ste5 molecules, the CoV of bound Ste5 molecules in the PSn_0 complex decreased and increased in both PSn_1 and PSn_2 complexes. **(b)** 30 Ptc1 and 5000 Fus3 molecules. By increasing the number of Ste5 molecules, the CoV of bound Ste5 molecules in both PSn_1 and PSn_2 complexes remained constant. The CoV of bound Ste5 molecules in the PSn_0 complex varied.

3.8 Fano factor for Ptc1 at 30 molecules

The fano factor of bound Ste5 molecules in the three different Ste5-Fus3 complexes for a Ptc1 value at 30 and Fus3 values at 100 and 5000 molecules were performed. The number of Ste5 was increased from 100 to 1500 molecules. By increasing the number of Ste5 molecules from 100 to 1500 at 30 Ptc1 and 100 Fus3 molecules (24a), the fano factor of bound Ste5 molecules in all three Ste5_Fus3 complexes increased. It increased from about 0,5 to 12 in the FSn_0 complex, from about 2 to 9 in the FSn_1 complex, and from about 2,4 to 16 in the FSn_2 complex. By increasing the number of Ste5 molecules from 100 to 1500 at 30 Ptc1 and 5000 Fus3 molecules (24b), the fano factor of bound Ste5 molecules in all three Ste-Fus3 complexes decreased. It decreased from about 0,5 to zero in the FSn_0 complex, from about 2,25 to 1,25 in the FSn_1 complex, and from about 2,7 to 1,5 in the FSn_2 complex. The fano factor of bound Ste5 molecules at 30 Ptc1 and 100 and 5000 Fus3 molecules can be seen in figure 14a-b, respectively.

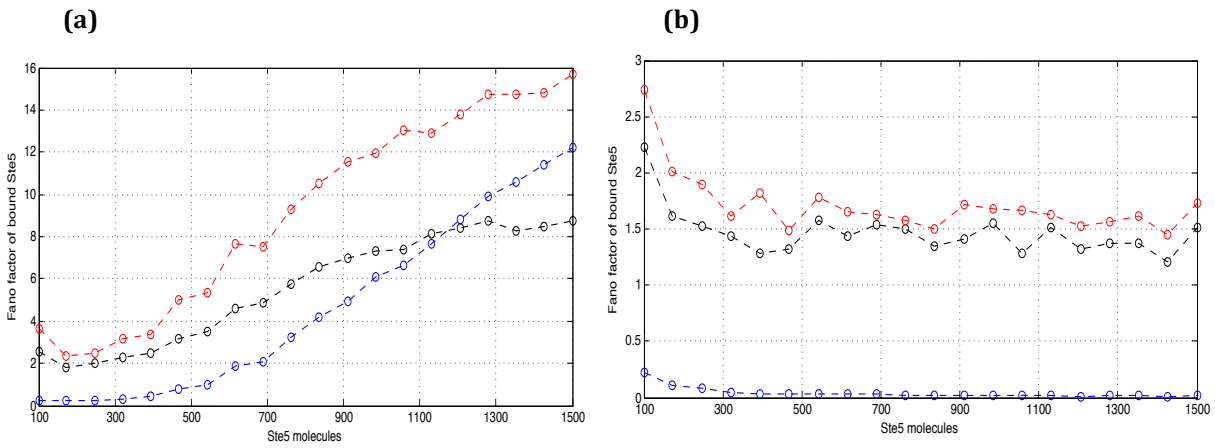

Figure 24. Fano factor of bound Ste5 molecules in the Ste5-Fus3 complexes. Fano factor of bound Ste5 molecules in FSn_0 (blue), FSn_1 (black), and FSn_2 (red) complexes at 30 Ptc1 and 100 and 5000 Fus3 molecules. The number of Ste5 increased from 100 to 1500 molecules. **(a)** 30 Ptc1 and 100 Fus3 molecules. By increasing the number of Ste5 molecules, the fano factor of bound Ste5 molecules in the three different St35-Fus3 complexes increased. (b) 30 Ptc1 and 5000 Fus3 molecules. By increasing the number of Ste5 molecules, the fano factor of bound Ste5 molecules in all the three Ste5-Fus3 complexes decreased.

The fano factor of bound Ste5 molecules in the three different Ste5-Ptc1 complexes for a Ptc1 value at 30 and Fus3 values at 100 and 5000 molecules were performed. The number of Ste5 was increased from 100 to 1500 molecules. By increasing the number of STe5 molecules from 100 to 1500 at 30 Ptc1 and 100 Fus3 molecules (25a), the fano factor of bound Ste5 molecules in the PSn_0 complex decreased from about 2 to 0,5. The fano factor value of bound Ste5 molecules in the PSn_1 complex decreased from 3 to 2 from 100 to 200 Ste5 molecules and further increased to 4. In the PSn_2 complex, the fano factor of bound Ste5 molecules decreased from 2 to 1 from 100 to 200 Ste5 molecules and further increased to 11. By increasing the number of Ste5 molecules at 30 Ptc1 and 5000 Fus3 molecules (25b), the fano factor of bound Ste5 molecules in the three Ste5_Ptc1 complexes decreased. It decreased from about 1 to 0,8 in the PSn_0 complex, from 2,3 to 1,3 in the PSn_1 complex, and from 1,3 to 0,3 in the PSn_2 complex. The fano factor of bound Ste5 molecules in the three different Ste5-Ptc1 complexes can be seen in figure 25a-b, respectively.

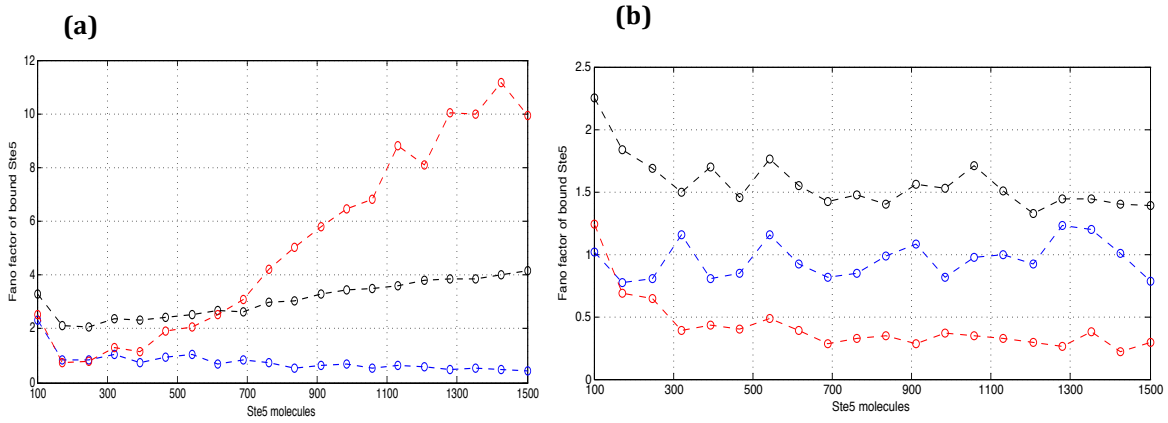

Figure 25. Fano factor of bound Ste5 molecules in the Ste5-Ptc1 complexes. Fano factor of bound Ste5 molecules in PSn_0 (blue), PSn_1 (black), and PSn_2 (red) complexes at 30 Ptc1 and 100 and 5000 Fus3 molecules. The number of Ste5 increased from 100 to 1500 molecules. (a) 30 Ptc1 and 100 Fus3 molecules. By increasing the number of Ste5 molecules, the fano factor of bound Ste5 molecules in both PSn_1 and PSn_2 complexes increased and decreased in the PSn_0 complex. (b) 30 Ptc1 and 5000 Fus3 molecules. By increasing the number of Ste5 molecules, the fano factor of bound Ste5 molecules in all the three Ste5-Fus3 complexes decreased.

3.9 Changing kinetic rates

The kinetic rates $f_1^{(K)}$ and $f_1^{(P)}$ were selected to be changed. In the nature article, the given value of the kinetic rate $f_1^{(K)}$ was 480 molecules per second and 7400 molecules per second for $f_1^{(P)}$, see Appendix A. It was performed four stochastic simulations with change values of the kinetic rates. The $f_1^{(K)}$ value was reduced to 10 molecules per second with 100 and 615 Fus3 molecules. Additionally the $f_1^{(P)}$ value was increased to 15000 molecules per second with 100 and 615 Fus3 molecules. The Ptc1 values in the four simulations were constant at 30 molecules. By decreasing the kinetic rate $f_1^{(K)}$ from 480 to 10 molecules per second, the mean of bound Ste5 in the Ste5-Fus3 and Ste5-Ptc1 complexes were calculated. It resulted in the same mean values of bound Ste5 in the Ste5-Fus3 and Ste5-Ptc1 complexes when the kinetic rates were not changed, figure 26-29. The kinetic rate $f_1^{(P)}$ were increased from 983 to 15000 molecules per second, and the mean of bound Ste5 in the Ste5-Fus3 and Ste5-Ptc1 complexes were calculated. Equal to the kinetic rate $f_1^{(K)}$, the changed value of $f_1^{(P)}$ did not differ from performed simulation with non-changed kinetic rates, figure 17 and 18. Due to this, the standard deviation, coefficient of variation, and fano factor were not calculated for stochastic simulations with changed values of the kinetic rates.

4. Discussion

4.1 General description of the system

The haploid yeast *S.cerevisiae* is assumed to be in three different states; an "off" state, a "switch" state, and an "on" state. Without any influence an a- or α-factor, no formation of the yeast can occur. By increasing the value of mating pheromone, more Ptc1 molecules can contribute in the competition of phosphorylation/dephosphorylating of the four phosphosites at the scaffold protein Ste5. To disrupt the Ste5-Fus3 complex and achieve a full activation of Fus3, all the phosphosites needs to be dephosphorylated of Ptc1. Hence, mating of the haploid yeast *S.cerevisiae* is possible. The "off" state indicates a steady state when the switch-like decision in yeast has occurred. The "on" state is set to be at 100 Fus3 molecules, the "switch" state is set to be at about 1100 Fus3 molecules (1131 in deterministic and 1188 in stochastic analysis), and the "off" state is set to be at 5000 Fus3 molecules.

4.2 Deterministic analysis

In the deterministic analysis, measurements of the system were performed at the steady state solutions du to it represent the system behavior after "some time has elapsed. In the steady state solutions, the initial fluctuations have died out. It was performed three simulations with a Ptc1 value at 30, 500, and 1000 molecules The number of Ste5 molecules was increased from 100 to 1500 and the value of Fus3 molecules was 100, 1188, and 5000 molecules. It was measured the amount of free Ste5 and bound Ste5 molecules in both Ste5-Fus3 and Ste5-Ptc1 complexes in the system.

In figure 16, it was measured the mean of free Ste5 in the S0, S1, S3, and S4 complexes. By increasing the number of Fus3 molecules, the mean of free Ste5 molecules in the system decreased due to an increase of bound Ste5 molecules in the Ste5-Fus3 and/or Ste5-Ptc1 complexes. By increasing the Ptc1 value, more Ste5 molecules were necessary to achieve free Ste5 molecules. The distribution of bound Ste5 molecules in the three different Ste5-Fus3 complexes and free Ste5 molecules with different Ptc1 and Fus3 values were measured and can be seen in figure 17. At 30 Ptc1 molecules, the "on" state with 100 Ste5 molecules resulted in a low amount of free Ste5 molecules and a high amount of bound Ste5 molecules. The bound Ste5 molecules were distributed in the three different Ste5_Fus3 complexes. In the "switch" state with 1131 Fus3 molecules, there were a higher amount of free Ste5 molecules in the system and it was needed a higher amount of Ste5 molecules to

achieve more bound Ste5 molecules. Most bound Ste5 molecules were in the FSn_0 complex. In the “off” state with 5000 Fus3 molecules, there were a low amount of bound Ste5 molecules in the FSn_0 complex and a high amount of free Ste5 molecules. Due to a reached steady state, the increased number of Ste5 molecules resulted in a low variation of the free and bound Ste5 molecules. At 500 Ste5 molecules in the “on” state at 100 Fus3 molecules, the mean of free Ste5 molecules needed a higher amount of Ste5 molecules to decrease likewise with the bound Ste5 molecules. By increasing the number of Ptc1 molecules, most Ste5 molecules were bound in the FSn_2 complex instead of the FSn_0 complex at 30 Ptc1 molecules. In the “switch” state with 1131 Ste5 molecules; free Ste5 molecules needed a higher amount of Ste5 molecules to increase as with bound Ste5 molecules. However, instead of most bound Ste5 molecules in the FSn_0 complex at 30 Ptc1 molecules, there were bound Ste5 molecules in the three Ste5-Fus3 complexes. At the “off” state with 500 Ste5 molecules, there was a slow decrease of free Ste5 and a slow increase of bound Ste5 molecules. It was a high amount of free Ste5 molecules in the system. By increasing the number of Ptc1 to 1000 molecules, the “on” state at 100 Fus3 molecules had a slower decrease of free Ste5 molecules and a slower increase of bound Ste5 molecules compares to the “on” state at 500 Ptc1 molecules. As in the “on” state with 500 Ptc1 molecules, the most bound Ste5 molecules at 1000 Ptc1 molecules were in the FSn_2 complex. In the “switch” state at 1131 Fus3 molecules, the most bound Ste5 molecules were in the FSn_2 complex, which had not been occurred at Ptc1 values at 30 and 500 molecules. Free Ste5 molecules had a slower decrease and bound Ste5 molecules had a slower increase at 1000 Ptc1 molecules than at lower Ptc1 values. In the “off” state at 5000 Fus3 molecules, the amount of free Ste5 and bound Fus3 molecules did note have a large change due to increased number of Ste5 molecules. The bound Ste5 molecules were mainly bound to FSn_2 complex.

The distribution of bound Ste5 molecules in the three different Ste5-Ptc1 complexes with different Ptc1 and Fus3 values were measured and can be seen in figure 17. With Ptc1 at 30 in the “on” state at 100 Fus3 molecules, both the mean of free and bound Ste5 molecules remained constant due to an increased number of Ste5 molecules. There were no free Ste5 molecules in the system and the most bound Ste5 molecules were in the PSn_2 complex. In the “switch” state at 1131 Fus3 molecules, it was no significant changes except a small amount of free Ste5 molecules with less than 200 Ste5 molecules. In the “off” state at 5000 Fus3 molecules, there were some free Ste5 molecules, but the Ste5 molecules were mainly bound in the PSn_2 complex. By increasing the number of Ptc1 molecules to 500, the “on” state at 100 Fus3 molecules had a high amount of free Ste5 molecules that had a slow

decrease. Ste5 molecules were bound in both the PSn_0 and PSn_2 complexes instead of only the PSn_2 complex at 30 Ptc1 molecules. At 500 Ptc1 molecules in the "switch" state at 1131 Fus3 molecules, there were more free Ste5 molecules in the system than with 30 Ptc1 molecules. The most bound Ste5 molecules were in the PSn_2 complex, same as for 30 Ptc1 molecules. In the "off" state at 5000 Ste5 and 500 Ste5 molecules, the most bound Ste5 molecules were in the PSn_2 complex, same as for Ptc1 value at 30 molecules. However, it was a high amount of free Ste5 molecules in the system that had a slow decrease. By increasing the number of Ptc1 molecules to 1000, the "on" state had a high amount of free Ste5 molecules as with 500 molecules. However, the Ste5 molecules had a slower decrease. As in the "off" state at 500 Ptc1 molecules, the bound Ste5 molecules were mainly in the PSn_0 and PSn_2 complexes. However the amount of bound Ste5 molecules in PSn_0 complex was three times higher than in the PSn_2 complex. In the "switch" state at 1131 Fus3 molecules and 1000 Ptc1 molecules, it was a higher amount of free Ste5 molecules. The mean of bound Ste5 molecules in both PSn_0 and PSn_1 complexes had increased, but the most bound Ste5 molecules were in the PSn_2 complex, same as for Ptc1 values at 30 and 500 molecules. In the "off" state at 5000 Ste5 molecules, it was a higher amount of free Ste5 molecules than at 30 and 500 Ptc1 molecules, but it had a slower decrease. Same as for Ptc1 at 30 and 500 molecules, the most bound Ste5 molecules were in the PSn_2 complex.

4.3 Stochastic analysis

Like the deterministic analysis, measurements of the system were performed at the steady state solutions where it represented the system behavior after "some time has elapsed. However, in the stochastic analysis there will be fluctuations in the steady state. To obtain a correct result in both the deterministic and stochastic analysis, the measurements in the simulations must be at the same place. Same as in the deterministic analysis, it was performed three simulations with a Ptc1 value at 30, 500, and 1000 molecules in the stochastic analysis. The number of Ste5 molecules was increased from 100 to 1500 and the value of Fus3 molecules was 100, 1131, and 5000 molecules. It was measured the amount of free Ste5 and bound Ste5 molecules in both Ste5-Fus3 and Ste5-Ptc1 complexes in the system.

The distribution of bound Ste5 molecules in the three different Ste5-Fus3 complexes and free Ste5 molecules with different Ptc1 and Fus3 values were measured and can be seen in figure 19. By increasing the number of Ptc1 molecules to 30, the "off" state at 100 Fus3

molecules had bound Ste5 molecules in the three Ste5-Fus3 complexes. Most bound Ste5 molecules were in the FSn_0 complex. It was only a small amount of free Ste5 molecules with a Ste5 value under 200. In the “switch” state at 1131 Fus3 molecules, it was a high amount of free Ste5 molecules that decreased due to an increased number of Ste5 molecules. All bound Ste5 molecules were in the FSn_0 complex. In the “off” state, it was a higher amount of free Ste5 molecules that had a slow decrease. The amount Ste5 molecules in the system were in the FSn_0 complex. By increasing the number of Ptc1 molecules to 500, the “on” state at 100 Ste5 molecules had a higher amount of free Ste5 molecules than a lower Ptc1 value at 30 molecules. There was a high amount of bound Ste5 molecules in the FSn_2 complex. In the “switch” state at 1131 Fus3 molecules, it about the same amount of free Ste5 molecules, but it had a slower decrease. There were bound Ste5 molecules in the three different Ste5-Fus3 complexes, but the FSn_0 complex had the highest amount of bound Ste5 molecules. In the “off” state at 5000 Fus3 molecules, it was a high amount of free Ste5 molecules same at 30 Ptc1 molecules, but it had a slower decrease. It was a decreased value of bound Ste5 molecules compared to “off” state at 30 Ptc1 molecules. However, the most bound Ste5 molecules were in the FSn_0 complex. By increasing the number of Pt1 molecules to 1000, the “on” state had about the same value of free Ste5 molecules, but it had a slower decrease. The value of bound Ste5 molecules was same as in the “off” state at 500 Ptc1 molecules with most bound Ste5 molecules in the FSn_2 complex. In the “switch” state at 1131 Fus3 molecules, the amount of free Ste5 molecules were the same for all the three different Ptc1 values. However, it had a slower decrease. Bound Ste5 molecules were mainly in the FSn_2 complex. In the “off” state, there was a high amount of free Ste5 molecules, same as in all the “off” states with different Ptc1 values. However, the amount of free Ste5 molecules had a slower decrease. In the “off” state at 30 and 500 Ptc1 molecules, the FSn_0 complex had the highest value of bound Ste5 molecules. However, at 1000 Ptc1 molecules the highest amount of bound Ste5 molecules was in the FSn_2 complex.

Due to similar distribution of bound Ste5 molecules in the Ste5-Ptc1 complexes, the measurements were not included. Hence, the distribution can be seen in the deterministic analysis in figure 18 and is explained in Sec. 4.2.

4.4 Bound Ste5 molecules in single complexes

The measurements of bound Ste5 in the three different Ste5-Fus3 and Ste5-Ptc1 complexes were performed with different Ptc1 and Fus3 values. In both analyses, the number of Ste5 molecules increased from 100 to 1500 and it was used Ptc1 values at 30, 500, and 1000 molecules. In the deterministic analysis, the Fus3 values at 100, 1188, and 5000 were used. The Fus3 values at 100, 1131, and 5000 molecules were used in the stochastic analysis. After measuring the mean of the three different Ste5-Fus3 and Ste5-Ptc1 complexes in the deterministic and stochastic analysis, most bound Ste5 molecules were located in the FSn_0 complex. The calculation of bound Ste5 molecules in single complexes were performed in order to evaluate the distribution of bound Ste5 molecules, Tabl. 2 and 3. In the deterministic analysis at 30 Ptc1 and 100 Fus3 molecules, the highest mean of bound Ste5 molecules was located in the FS4_0 complex at 72 molecules. At 30 Ptc1 and 5000 Fus3 molecules, the highest mean of bound Ste5 molecules was located in the FS4_0 complex at 757 molecules. In the stochastic analysis at 30 Ptc1 and 100 Fus3 molecules, the highest mean of bound Ste5 molecules was located in the FS4_0 complex at 72 molecules. At 30 Ptc1 and 5000 Fus3 molecules, the highest mean of bound Ste5 molecules was located in the FS4_0 complex at 757 molecules. By comparing the calculations of bound Ste5 molecules in single molecules in deterministic and stochastic analysis, the highest mean of bound Ste5 molecules were located in the FS4_0 complex due to increased Fus3 values.

4.5 Fluctuations

The system was explored further by exposing it to stochastic fluctuations. By this, it is possible to verify the bistable regions and the stability of stable steady states. Measuring of the standard deviation, coefficient of variation, and fano factor in the stochastic analysis were performed to analyze the dispersion in the system. The standard deviation of bound Ste5 molecules in the Ste5-Fus3 and Ste5-Ptc1 complexes can be seen in figure 20 and 21.

The standard deviation in the three different Ste5-Fus3 complexes for a Ptc1 value at 30 and Fus3 values at 100 and 5000 molecules were performed. The number of Ste5 was increased from 100 to 1500 molecules. By increasing the number of Ste5 molecules from 100 to 1500, the standard deviation of bound Ste5 molecules increased in the three Ste5-Fus3 complexes. At 100 Ste5 molecules, the three Ste5-Fus3 complexes had the same standard

deviation, but it varied due to an increased number of Ste5 molecules. The FSn_0 complex had the highest standard deviation, which increased from 5 to 25. The FSn_1 complex had the lowest standard deviation, which increased form 5 to about 15. By increasing the Fus3 value from 100 to 500, overall standard deviation of the three Ste5-Fus3 complexes decreased. The standard deviation for the FSn_0 complex varied from 3,7 to 4,5, and the standard deviation in the FSn_2 complex varied from 2,5 to 3,3. By calculating the standard deviation, the value visualized the dispersion of the mean in the system. It is assumed that there are some correlations in the system, but since the covariance values were not calculated, this is difficult to claim. It was performed some covariance calculations, but the values were not zero. However, the standard deviation equation with correlations was used by assuming that the covariance values were zero. Hence, the values will be the lower boundary or estimate of the actually standard deviation for the combined values. Hence, by increasing the Fus3 values, it is less dispersion of the mean values. Additionally, the standard deviation of bound Ste5 molecules in the three different Ste5-ptc1 complexes for at Ptc1 value at 30 and Fus3 values 100 and 5000 molecules were performed. The number of Ste5 was increased from 100 to 1500 molecules. The standard deviation of 100 Fus3 resulted in a constant value for the PSn_0 complex at 1, and a constant value at 2 for the PSn_1 complex. For the PSn_2 complex, the standard deviation value increased from about 5 to 18. By increasing the Fus3 value from 100 to 5000 molecules, the standard deviation values in the PSn_2 complex decreased from 5,5 to 2,5. The standard deviation in the PSn_0 complex remained the same, and decreased from 2 to 1,5 in the PSn_1 complex.

The coefficient of variation (CoV) measures the relations between the standard deviation and mean. Measured CoV of bound Ste5 molecules in the Ste5-Fus3 and Ste5_Ptc1 complexes can be seen in figure 22 and 23. The CoV in the three different Ste5-Fus3 complexes for a Ptc1 value at 30 and Fus3 values at 100 and 5000 molecules were performed. The number of Ste5 was increased from 100 to 1500 molecules. By increasing the number Fus3 molecules to 100, the CoV of bound Ste5 molecules in the FSn_0 complex increased from about 0,05 to 0,5. The CoV of bound Ste5 molecules in the FSn_1 complex varied from 0,45 to 0,65, and from about 0,7 to 1 in the FSn_2 complex. By increasing the number of Fus3 molecules from 100 to 5000, the CoV of bound Ste5 molecules in FSn_0 complex decreased from 0,05 to zero, from 0,6 to 0,4 in the FSn_1 complex, and from 0,85 to about 0,6 in the FSn_2 complex. Hence, increased number of Fus3 molecules resulted in increased relation between the standard deviation and mean. Additionally, it was measured the CoV of bound Ste5 molecules in the three different Ste5-Ptc1 complexes for a Ptc1 value at 30 and

Fus3 values at 100 and 5000 molecules. The number of Ste5 was increased from 100 to 1500 molecules. By increasing the number of Fus3 molecule to 100, the CoV of bound Ste5 molecules in the PSn_0 complex decreased from 5,5 to 1. The CoV of bound Ste5 molecules in the PSn_1 complex increased from 1,5 to 1,8, and increased from 0,2 to 0,5 in the PSn_2 complex. By increasing the number of Fus3 molecules from 100 to 5000, the CoV of bound Ste5 molecules in the both PSn_1 and PSn_2 complexes remained constant at 1,5 and 0,2. For the PSn_0 complex, the CoV varied from about 5 to 8. Hence, by increasing the number of Fus3 molecules, the dispersion between the standard deviation and mean in both PSn_1 and PSn_2 complexes decreased, and increased in the PSn_0 complex.

The fano factor measures the relations between the CoV multiplied with the standard deviation. Measured fano factor of bound Ste5 molecules in the Ste5-Fus3 and Ste5-Ptc1 complexes can be seen in figure 24 and 25. The fano factor of bound Ste5 molecules in the three different Ste5-Fus3 complexes for a Ptc1 value at 30 and Fus3 values at 100 and 5000 molecules were performed. The number of Ste5 was increased from 100 to 1500 molecules. By increasing the number Fus3 to 100, the fano factor of bound Ste5 molecules in all three Ste5-Fus3 complexes were increased. It increased from about 0,5 to 12 in the FSn_0 complex, from t 2 to 9 in the FSn_1 complex, and from 2,4 to 16 in the FSn_2 complex. By further increasing the number of Fus3 molecules from 100 to 5000 molecules, the fano factor of bound Ste5 molecules in all three Ste-Fus3 complexes decreased. It decreased from about 0,5 to zero in the FSn_0 complex, from about 2,25 to 1,25 in the FSn_1 complex, and from about 2,7 to 1,5 in the FSn_2 complex. The fano factor of bound Ste5 molecules in the three different Ste5-Ptc1 complexes for a Ptc1 value at 30 and Fus3 values at 100 and 5000 molecules were performed. The number of Ste5 was increased from 100 to 1500 molecules. By increasing the number of Ste5 molecules to 100, the fano factor of bound Ste5 molecules in the PSn_0 complex decreased from about 2 to 0,5. The fano factor value of bound Ste5 molecules in the PSn_1 complex increased from about 2 to 4, and increased from about 1 to 11 in the PSn_2 complex. By further increasing the number of Fus3 from 100 to 5000 molecules, the fano factor of bound Ste5 molecules in the three Ste5-Ptc1 complexes decreased. It decreased from about 1 to 0,8 in the PSn_0 complex, from 2,3 to 1,3 in the PSn_1 complex, and from 1,3 to 0,3 in the PSn_2 complex. Hence, by increasing the number of Fus3 molecules from 100 to 5000, the dispersion of fluctuations is decreased.

4.6 Kinetic rates

It was performed stochastic simulations with changed kinetic rates with 30 Ptc1, 100 and 615 Fus3 molecules. In Malleshaiah et al. (Malleshaiah et al., 2010), the value of $f_1^{(K)}$ was set to be 480 molecules per liter and the value of $f_1^{(P)}$ to be 7400 molecules per second, Appendix C. The kinetic rate $f_1^{(K)}$ was decreased to 10 molecules per second and the $f_1^{(K)}$ was increased to 15000 molecules per second. Despite changed kinetic rate values, the mean of free and bound Ste5 molecules remained the same as for stochastic simulations where the kinetic rates were not changed. This result may indicate that the kinetic rates are robust in the system. Hence, by being robust they maintain their functions in the system despite external and internal perturbations (Kitano, 2004). In Malleshaiah et al. (2010) the errors of the kinetic rates indicated the coefficient of variation. This represents the ration between the standard deviation and mean of the parameters over a Monte Carlo run, where they were restricted to vary only within a factor of 2 from their best-fit values. By using a Monte Carlo method, a random sample is repeated to obtain numerical results. The simulations are run many times in order to calculate those same probabilities (Kalos and Whitlock, 2008). The error of the kinetic rate $f_1^{(K)}$ was 24% and 35% for the $f_1^{(P)}$. The standard deviation values indicate that it was not a large dispersion of the values for the kinetic rates. However, the results were given by performing a deterministic simulation, which do not take stochastic processes into account. In the thesis, it was included the stochastic processes, but the results did not differ from the deterministic simulations. Hence, the system was robust.

4.7 Future prospects/future directions

For this modified model there are many interesting features that could be tested. The calculation of single complexes has only been performed for two different Fus3 values at 100 and 5000 molecules at 30 Ptc1 molecules. It could be performed calculations for several Fus3 and Ptc1 values. Calculating the mean of free Ste5 and bound Ste5 molecules with different Fus3 and Ptc1 values. The number of Ste5 molecules was set to range from 100 to 1500 molecules, but this value could be increased. Additionally, only two kinetic rates were changed. The kinetic rates could be calculated with different values or other kinetic rates could be changed.

5. Conclusion

The model of a switch-like mating decision in the haploid yeast *S. cerevisiae* from Malleshaiah et. al. (2010) was modified in order to perform both deterministic and stochastic analysis. Deterministic analysis was conducted with mean measurements. Furthermore, stochastic simulation of the modified model was conducted. Hence, it was possible to analyze the fluctuations in the system by calculating the mean, standard deviation, coefficient of variation and fano factor. This gave an indication of the switch. It was calculated the mean values of free and bound Ste5 molecules and the amount in every single complexes. Due to an increase of the Ste5 and Fus3 molecules, the mean of free and bound Ste5 molecules were changed. By calculating the mean of bound Ste5 molecules in single complexes, the distribution of bound Ste5 molecules was about the same. The parameter values were conducted from literature, which were used in both the deterministic and stochastic simulations. The system was not affected by kinetic rate changes. Hence, it was robust.

6. References

ALBERTS, B. 2008. *Molecular Biology of the Cell*, Garland Science.

ANDRIANANTOANDRO, E., BASU, S., KARIG, D. K. & WEISS, R. 2006. Synthetic biology: new engineering rules for an emerging discipline. *Molecular systems biology,* 2.

ATTAWAY, S. 2011. *MATLAB: A practical introduction to programming and problem solving*, Butterworth-Heinemann.

BARDWELL, L. 2005. A walk-through of the yeast mating pheromone response pathway. *Peptides,* 26**,** 339-350.

BROWN, C. 1998. Coefficient of Variation. *Applied Multivariate Statistics in Geohydrology and Related Sciences.* Springer Berlin Heidelberg.

ELION, E. A. 2000. Pheromone response, mating and cell biology. *Current Opinion in Microbiology,* 3**,** 573-581.

ELOWITZ, M. B. & LEIBLER, S. 2000. A synthetic oscillatory network of transcriptional regulators. *Nature,* 403**,** 335-338.

FU, P. & PANKE, S. 2009. *Systems biology and synthetic biology / edited by Pengcheng Fu, Sven Panke*, John Wiley & Sons.

GARDNER, T. S., CANTOR, C. R. & COLLINS, J. J. 2000. Construction of a genetic toggle switch inEscherichia coli. *Nature,* 403**,** 339-342.

GIBSON, M. A. & BRUCK, J. 2000. Efficient exact stochastic simulation of chemical systems with many species and many channels. *The journal of physical chemistry A,* 104**,** 1876-1889.

GILLESPIE, D. T. 1976. A general method for numerically simulating the stochastic time evolution of coupled chemical reactions. *Journal of computational physics,* 22**,** 403-434.

GILLESPIE, D. T. 1977. Exact stochastic simulation of coupled chemical reactions. *The journal of physical chemistry,* 81**,** 2340-2361.

HUANG, D. C., HOLTZ, W. J. & MAHARBIZ, M. M. 2012. A genetic bistable switch utilizing nonlinear protein degradation. *Journal of biological engineering,* 6**,** 9.

JORGENSEN, P., NISHIKAWA, J. L., BREITKREUTZ, B.-J. & TYERS, M. 2002. Systematic identification of pathways that couple cell growth and division in yeast. *Science Signaling,* 297**,** 395.

KALOS, M. H. & WHITLOCK, P. A. 2008. *Monte carlo methods*, Wiley-VCH.

KARLEBACH, G. & SHAMIR, R. 2008. Modelling and analysis of gene regulatory networks. *Nature Reviews. Molecular Cell Biology,* 9**,** 770-80.

KITANO, H. 2002a. Computational systems biology. *Nature,* 420**,** 206-210.

KITANO, H. 2002b. Systems biology: A brief overview. *Science,* 295**,** 1662-4.

KITANO, H. 2004. Biological robustness. *Nature Reviews Genetics,* 5**,** 826-837.

KLIPP, E., LIEBERMEISTER, W., WIERLING, C., KOWALD, A., LEHRACH, H. & HERWIG, R. 2011. *Systems Biology,* Weinheim, John Wiley & Sons.

KOFAHL, B. & KLIPP, E. 2004. Modelling the dynamics of the yeast pheromone pathway. *Yeast (Chichester, England),* 21**,** 831-850.

KÆRN, M., ELSTON, T. C., BLAKE, W. J. & COLLINS, J. J. 2005. Stochasticity in gene expression: from theories to phenotypes. *Nature Reviews Genetics,* 6**,** 451-464.

MACKAY, V. & MANNEY, T. R. 1974a. Mutations affecting sexual conjugation and related processes in Saccharomyces cerevisiae. I. Isolation and phenotypic characterization of nonmating mutants. *Genetics,* 76**,** 255-271.

MACKAY, V. & MANNEY, T. R. 1974b. Mutations affecting sexual conjugation and related processes in Saccharomyces cerevisiae. II. Genetic analysis of nonmating mutants. *Genetics,* 76**,** 273-288.
MALLESHAIAH, M. K., SHAHREZAEI, V., SWAIN, P. S. & MICHNICK, S. W. 2010. The scaffold protein Ste5 directly controls a switch-like mating decision in yeast. *Nature,* 465**,** 101-5.
MCADAMS, H. H. & ARKIN, A. 1997. Stochastic mechanisms in gene expression. *Proceedings of the National Academy of Sciences,* 94**,** 814-819.
MONTELONE, B. A. 2002. Yeast mating type. *eLS*.
MYERS, C. J. 2009. Engineering genetic circuits. *Scitech Book News.* Portland, United States, Portland: Book News, Inc.
POMERENING, J. R. 2008. Uncovering mechanisms of bistability in biological systems. *Current Opinion in Biotechnology,* 19**,** 381-388.
STROGATZ, S. 2001. Nonlinear dynamics and chaos: with applications to physics, biology, chemistry and engineering.
VOIT, E. O. 2013. *A first course in systems biology,* New York, Garland Science.
ZULLIGER, H. & AITKEN, D. 1970. Fano factor fact and fallacy. *Nuclear Science, IEEE Transactions on,* 17**,** 187-195.

Appendix A

Table A1. Reactions for modified model. The reactions set consist of total 76 reactions. The table is divided into two columns, Fus3 and Ptc1, with their corresponding equations and rate constants.

Fus3	Ptc1
$S4 + F \xrightarrow{f1K\_F3} FS4\_0$	$S4 + P \xrightarrow{f1P\_P1} PS4\_0$
$S3 + F \xrightarrow{f1K\_F3} FS3\_0$	$S3 + P \xrightarrow{f1P\_P1} PS3\_0$
$S2 + F \xrightarrow{f1K\_F3} FS2\_0$	$S2 + P \xrightarrow{f1P\_P1} PS2\_0$
$S1 + F \xrightarrow{f1K\_F3} FS1\_0$	$S1 + P \xrightarrow{f1P\_P1} PS1\_0$
$S0 + F \xrightarrow{f1K\_F3} FS0\_0$	$S0 + P \xrightarrow{f1P\_P1} PS0\_0$
$FS4\_0 \xrightarrow{b4K} S4 + F$	$PS4\_0 \xrightarrow{b1P} S4 + P$
$FS3\_0 \xrightarrow{b3K} S3 + F$	$PS3\_0 \xrightarrow{b1P} S3 + P$
$FS2\_0 \xrightarrow{b2K} S2 + F$	$PS2\_0 \xrightarrow{b1P} S2 + P$
$FS1\_0 \xrightarrow{b1K} S1 + F$	$PS1\_0 \xrightarrow{b1P} S1 + P$
$FS0\_0 \xrightarrow{b0K} S0 + F$	$PS0\_0 \xrightarrow{b1P} S0 + P$
$FS3\_1 \xrightarrow{b4K} FS3\_2$	$PS4\_1 \xrightarrow{b1P} PS4\_2$
$FS2\_1 \xrightarrow{b3K} FS2\_2$	$PS3\_1 \xrightarrow{b1P} PS3\_2$
$FS1\_1 \xrightarrow{b2K} FS1\_2$	$PS2\_1 \xrightarrow{b1P} PS2\_2$
$FS0\_1 \xrightarrow{b1K} FS0\_2$	$PS1\_1 \xrightarrow{b1P} PS1\_2$
$FS3\_2 \xrightarrow{f3K} FS3\_1$	$PS4\_2 \xrightarrow{f3P} PS4\_1$
$FS2\_2 \xrightarrow{f3K} FS2\_1$	$PS3\_2 \xrightarrow{f3P} PS3\_1$
$FS1\_2 \xrightarrow{f3K} FS1\_1$	$PS2\_2 \xrightarrow{f3P} PS2\_1$
$FS0\_2 \xrightarrow{f3K} FS0\_1$	$PS1\_2 \xrightarrow{f3P} PS1\_1$
$FS3\_1 \xrightarrow{KK} FS4\_0$	$PS4\_1 \xrightarrow{KP} PS3\_0$
$FS2\_1 \xrightarrow{KK} FS3\_0$	$PS3\_1 \xrightarrow{KP} PS2\_0$
$FS1\_1 \xrightarrow{KK} FS2\_0$	$PS2\_1 \xrightarrow{KP} PS1\_0$
$FS0\_1 \xrightarrow{KK} FS1\_0$	$PS1\_1 \xrightarrow{KP} PS0\_0$

$FS3\_1 \xrightarrow{b6K} FS3\_0$ $FS2\_1 \xrightarrow{b6K} FS2\_0$ $FS1\_1 \xrightarrow{b6K} FS1\_0$ $FS0\_1 \xrightarrow{b6K} FS0\_0$	$PS4\_1 \xrightarrow{b2P} PS4\_0$ $PS3\_1 \xrightarrow{b2P} PS3\_0$ $PS2\_1 \xrightarrow{b2P} PS2\_0$ $PS1\_1 \xrightarrow{b2P} PS1\_0$
$FS0\_0 \xrightarrow{4f2K} FS0\_1$ $FS1\_0 \xrightarrow{3f2K} FS1\_1$ $FS2\_0 \xrightarrow{2f2K} FS2\_1$ $FS3\_0 \xrightarrow{f2K} Fs3\_1$	$PS4\_0 \xrightarrow{4f2P} PS4\_1$ $PS3\_0 \xrightarrow{3f2P} PS3\_1$ $PS2\_0 \xrightarrow{2f2P} PS2\_1$ $PS1\_0 \xrightarrow{f2P} PS1\_1$
$FS3\_2 \xrightarrow{KK} S4 + F$ $FS2\_2 \xrightarrow{KK} S3 + F$ $FS1\_2 \xrightarrow{KK} S2 + F$ $FS0\_2 \xrightarrow{KK} S1 + F$	$PS4\_2 \xrightarrow{KP} S3 + P$ $PS3\_2 \xrightarrow{KP} S2 + P$ $PS2\_2 \xrightarrow{KP} S1 + P$ $PS1\_2 \xrightarrow{KP} S0 + P$
$FS3\_2 \xrightarrow{b6K} S3 + F$ $FS2\_2 \xrightarrow{b6K} S2 + F$ $FS1\_2 \xrightarrow{b6K} S1 + F$ $FS0\_2 \xrightarrow{b6K} S0 + F$	$PS4\_2 \xrightarrow{b2P} S4 + P$ $PS3\_2 \xrightarrow{b2P} S3 + P$ $PS2\_2 \xrightarrow{b2P} S2 + P$ $PS1\_2 \xrightarrow{b2P} S1 + P$

Appendix B

Total set of nine ODEs describing the chemical reactions in the modified model.

$$\frac{dP}{dt} = b_1^{(P)} \cdot \sum_{n=0}^{4} PS_{n,0} - f_1^{(P)} \cdot P \cdot \sum_{n=0}^{4} S_n + \left(k^{(P)} + b_2^{(P)}\right) \cdot \sum_{n=1}^{4} PS_{n,2}\,. \tag{22}$$

$$\frac{dF}{dt} = \sum_{n=0}^{4} \cdot b_n^{(K)} \cdot FS_{n,0} - f_1^{(K)} \cdot F \cdot \sum_{n=0}^{4} S_n + \left(k^{(K)} + b_6^{(K)}\right) \cdot \sum_{n=1}^{3} FS_{n,2}\,. \tag{23}$$

$$\begin{aligned}\frac{dS_n}{dt} = {} & b_n^{(K)} \cdot FS_{n,0} - f_1^{(K)} \cdot F \cdot S_n + b_1^{(P)} \cdot PS_{n,0} - f_1^{(P)} \cdot P \cdot S_n + k^{(K)} \cdot FS_{(n-1),2} \\ & \cdot \theta\left(n - \frac{1}{2}\right) + k^{(P)} \cdot PS_{(n+1),2} \cdot \theta\left(\frac{7}{2} - n\right) + b_6^{(K)} \cdot FS_{n,2} \cdot \theta\left(\frac{7}{2} - n\right) + b_2^{(P)} \\ & \cdot PS_{n,0} \cdot \theta\left(n - \frac{1}{2}\right).\end{aligned} \tag{24}$$

$$\begin{aligned}\frac{dFS_{n,0}}{dt} = {} & f_1^{(K)} \cdot F \cdot S_n - b_n^{(K)} \cdot FS_{n,0} - (4-n) \cdot f_2^{(K)} \cdot FS_{n,0} \cdot \theta\left(\frac{7}{2} - n\right) + b_6^{(K)} \cdot FS_{n,1} \\ & \cdot \theta\left(\frac{7}{2} - n\right) + k^{(K)} \cdot FS_{(n-1),1} \cdot \theta\left(n - \frac{1}{2}\right).\end{aligned} \tag{25}$$

$$\begin{aligned}\frac{dPS_{n,0}}{dt} = {} & f_1^{(P)} \cdot P \cdot S_n - b_1^{(P)} \cdot PS_{n,0} - n \cdot f_2^{(P)} \cdot PS_{n,0} \cdot \theta\left(n - \frac{1}{2}\right) + b_2^{(P)} \cdot PS_{n,1} \\ & \cdot \theta\left(n - \frac{1}{2}\right) + k^{(P)} \cdot PS_{(n+1),1} \cdot \theta\left(\frac{7}{2} - n\right).\end{aligned} \tag{26}$$

$$\frac{dFS_{n,1}}{dt} = (4-n) \cdot f_2^{(K)} \cdot FS_{n,0} - \left(b_6^{(K)} - b_n^{(K)}\right) \cdot FS_{n,1} - k^{(K)} \cdot FS_{(n+1),1} + f_3^{(K)} \cdot FS_{n,2}. \tag{27}$$

$$\frac{dPS_{n,1}}{dt} = n \cdot f_2^{(P)} \cdot PS_{n,0} + \left(b_2^{(P)} - k^{(P)} - b_1^{(P)}\right) \cdot PS_{n,1} + f_3^{(P)} \cdot PS_{n,2}. \tag{28}$$

$$\frac{dFS_{n,2}}{dt} = b_b^{(K)} \cdot FS_{n,1} + \left(-f_3^{(K)} - k^{(K)} - b_b^{(K)}\right) \cdot FS_{n,2}. \tag{29}$$

$$\frac{dPS_{n,2}}{dt} = b_1^{(P)} \cdot PS_{n,1} + \left(-f_3^{(P)} - k^{(P)} - b_2^{(P)}\right) \cdot PS_{n,2}. \tag{30}$$

Appendix C

Table C1. Concentration and number of molecules values for species. The concentration is in nanomolar (nM).

Species (parameter)	Concentration (nM)	Number of molecules
$Ste5_{tot}$	52	1310
$Fus3_{tot}$	197	4963
$Ptc1_{max}$	39	983
$Ptc1_{zero}$	1.2	30

Table C2. Kinetic rates from the nature article and the modified model with the corresponding values. The value of the kinetic rates is given in molecules per second (s^{-1}).

Kinetic rates in nature article	Kinetic rates in modified model	Value (s^{-1})
$f_1^{(P)}$	f1P•P	7400
$nf_2^{(P)}$	n•f2P	327
$f_3^{(P)}$	f3P	0.3
$b_1^{(P)}$	b1P	22
$b_2^{(P)}$	b2P	0.12
$f_1^{(K)}$	f1K•F	480
$f_2^{(K)}$	n•f2K	850
$f_3^{(K)}$	f3K	0.1
$b_1^{(K)}$	b0K	99
$b_2^{(K)}$	b1K	42
$b_3^{(K)}$	b2K	21
$b_4^{(K)}$	b3K	13
$b_5^{(K)}$	b4K	10
$b_6^{(K)}$	b6K	24
$k^{(K)}$	KK	1.13
$k^{(P)}$	KP	0.5